Global phase portraits of the quadratic systems having a singular and irreducible invariant curve of degree 3

J. Llibre

Departament de Matemàtiques, Universitat Autònoma de Barcelona,
Edifici C, 08193 Bellaterra, Barcelona, Catalonia, Spain
jllibre@mat.uab.cat

C. Pantazi

Departament de Matemàtiques, Universitat Politècnica de Catalunya,
(EPSEB), Av. Doctor Marañón, 44–50, 08028 Barcelona, Spain
chara.pantazi@upc.edu

Any singular irreducible cubic curve (or simply, cubic) after an affine transformation can be written as either $y^2 = x^3$, or $y^2 = x^2(x+1)$, or $y^2 = x^2(x-1)$. We classify the phase portraits of all quadratic polynomial differential systems having the invariant cubic $y^2 = x^2(x+1)$. We prove that there are 63 different topological phase portraits for such quadratic polynomial differential systems. We control all the bifurcations among these distinct topological phase portraits. These systems have no limit cycles. Only 3 phase portraits have a center, 19 of these phase portraits have one polycycle, 3 of these phase portraits have 2 polycycles. The maximum number of separartices that have these phase portraits is 26 and the minimum number is 9, the maximum number of canonical regions of these phase portraits is 7 and the minimum is 3.

Keywords: Poincaré disk, global phase portrait, singular curve, cubic curve, polycycles, canonical regions, separatrices.

1. Introduction and statement of the main result

Quadratic polynomial differential systems (or simply *quadratic systems*) are systems that can be written into the form

$$\dot{x} = P(x,y) = P_0 + P_1 + P_2, \qquad \dot{y} = Q(x,y) = Q_0 + Q_1 + Q_2, \tag{1}$$

where P_i and Q_i are real polynomials of degree i in the variables (x,y) and $P_2^2 + Q_2^2 \neq 0$.

An extensive literature is dedicated to the study of the quadratic systems these last years. For a good survey see the book of Reyn [Reyn, 1994] or the book of Artés et.al [Artés *et al.*, 2021], and references therein. For example, the following families of quadratic systems have been studied: homogeneous [Coll *et al.*, 1987], semi-homogeneous [Cairó & Llibre, 1997], bounded [Dickson *et al.*, 1970], reversible [Gavrilov & Iliev, 2000; Coll *et al.*, 2009], Hamiltonian [Artés & Llibre, 1994a; Chow *et al.*, 2002], Lienard [Dumortier & Li, 1997], integrable using Carleman and Painlevé tools [Hua *et al.*, 1996], rational integrable [Artés *et al.*, 2007, 2010, 2009], the ones having a star nodal point [Berlinski, 1966], a center [Vulpe, 1983; Lunkevich & Sibirskii, 1982; Coll *et al.*, 2009; Vulpe, 1983], one focus and one antisaddle [Artés & Llibre, 1994b], with a semi–elementary triple node [Artés *et al.*, 2013], chordal [Gasull *et al.*, 1986; Gasull & Llibre, 1988], with

four infinite singular points and one invariant straight line [Roset, 1991], with invariant lines [Schlomiuk & Vulpe, 2008a], and so on.

It is interesting to mention some results on the quadratic polynomial differential systems having invariant curves of degree less than three. First we introduce some notation. By $QSL_{\geq i}$ we denote the family of non-degenerate quadratic differential systems possessing invariant lines of total multiplicity at least i. By QSL_i we denote the family of non-degenerate quadratic differential systems possessing invariant lines of total multiplicity exactly i. By QSH we mean the family of non-degenerate quadratic differential systems possessing an invariant hyperbola. By QSE we mean the family of non-degenerate quadratic differential systems possessing an invariant ellipse. The results are: On $QSL_{\geq 5}$ the geometrical classification is done in [Scholomiuk & Vulpe, 2004], its topological classification (phase portraits) and the integrability is done in [Schlomiuk & Vulpe, 2008b]. On QSL_4 the geometrical classification is done in [Schlomiuk & Vulpe, 2008c], its topological classification (phase portraits) and the integrability is done in [Schlomiuk & Vulpe, 2008d]. Both geometrical and topological classification of the family of quadratic systems with the line at infinity filled up with singularities was done in the following paper (each system in this family has total multiplicity of finite invariant lines equal to 3 and the line at infinity is also invariant, see [Schlomiuk & Vulpe, 2008e]. On QSL_3 and hence on $QSL_{\geq 3}$ the geometrical classification is done in [Schlomiuk & Vulpe, 2010], and the topological classification (phase portraits) was done in [Schlomiuk & Vulpe, 2012; Schlomiuk & Zhang, 2018]. On QSH the geometrical classification was done in [Oliveira et al., 2017], the topological classification and the integrability of families in this class is done in [Oliveira et al., 2021a,b]. Additional references on quadratic polynomial differential where important global tools were introduced and used in studied of two families of quadratic differential systems are [Llibre & Schlomiuk, 2004; Artés et al., 2006].

There is also an extensively literature about Hilbert's sixteen problem and quadratic systems, see for example [Chen et al., 2006; Gavrilov, 2001; Li & Llibre, 2004; Li & Zhang, 2002; Lunkevich & Sibirskii, 1982; Zhang, 2002], and the notion of ciclicity [Żołądek, 1995; Han & Yang, 2005; Chow et al., 2002], and so on. For the study of some geometric properties of quadratic systems see [Roussarie & Schlomiuk, 2002; Schlomiuk & Vulpe, 2005], and others. In particular we pay attention on reference [Llibre et al., 2000] where the authors present a classification of all quadratic systems having one real reducible invariant algebraic curve of degree 3.

In [Bix, 2006] it is proved that a cubic algebraic curve (or simply a cubic) is singular and irreducible if and only if it can be written after affine transformations into one of the forms (See Figure 1).

$$y^2 = x^3, \qquad y^2 = x^2(x+1), \qquad y^2 = x^2(x-1).$$

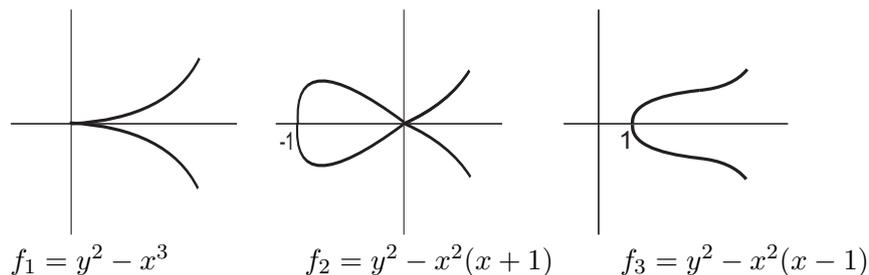$$f_1 = y^2 - x^3 \qquad f_2 = y^2 - x^2(x+1) \qquad f_3 = y^2 - x^2(x-1)$$

Fig. 1: Singular and irreducible algebraic curves of degree 3.

The goal of this paper is to continue the classification of the phase portraits in the Poincaré disc of the quadratic systems having some invariant cubic. Thus our main result is to provide all distinct topological phase portraits of the quadratic systems having the invariant cubic $y^2 = x^2(x+1)$.

Let $f = f(x,y) = 0$ be a real polynomial. We say that $f = 0$ is an invariant algebraic curve of system

(1) if it satisfies

$$P\frac{\partial f}{\partial x} + Q\frac{\partial f}{\partial y} = Kf,$$

for some polynomial K called the *cofactor* of the curve $f = 0$. Note that an invariant algebraic curve is formed by orbits of system (1).

By simple calculation we obtain the following:

Proposition 1. *The quadratic systems* (1) *having* $f = y^2 - x^2(x+1) = 0$ *as invariant algebraic curve are*

$$\begin{aligned}
\dot{x} &= ax + by + ax^2 + (3b - 2c)xy, \\
\dot{y} &= bx + ay + cx^2 + \frac{3}{2}axy + \left(\frac{9}{2}b - 3c\right)y^2.
\end{aligned} \tag{2}$$

See the Appendix for a summary of about the *Poincaré compactification* of a polynomial differential system and the definition of the *Poincaré disc* $\mathbb{D}$, which roughly speaking is to identify the interior of the unit closed disc $\mathbb{D}$ centered at the origin with the plane $\mathbb{R}^2$ and its boundary $\mathbb{S}^1$ with the infinity of $\mathbb{R}^2$, in the plane we can go to infinity in as many as directions as points has the circle $\mathbb{S}^1$. Then the Poincaré compactification consists in extend the quadratic differential system from the interior of $\mathbb{D}$ to its boundary $\mathbb{S}^1$, i.e. to the infinity of $\mathbb{R}^2$. In this way we can control the orbits of a polynomial differential in a neighborhood of the infinity, and in particular of a quadratic system.

As it is usual a *polycycle* is formed by a finite number of orbits $\gamma_1, \ldots, \gamma_n$ and a finite number of singular points $p_1, \ldots, p_n$ such that $\alpha(\gamma_i) = p_i$, $\omega(\gamma_i) = p_{i+1}$ for $i = 1, \ldots, n-1$, $\alpha(\gamma_n) = p_n$ and $\omega(\gamma_n) = p_1$. Possibly, some of the singular points p_i are identified.

Our main result is the following.

Theorem 1. *The following statements hold for the quadratic polynomial differential systems* (2).

(a) *There are* 63 *topological distinct phase portraits in the Poincaré disc. These* 63 *phase portraits are numbering as* pp_k *for* $k = 1, \cdots, 63$ *in what follows.*

(b) *These phase portraits have no limit cycles.*

(c) *The phase portraits* pp_k *for* $k = 2, 4, 5$ *have a center.*

(d) *The phase portraits* pp_k *for* $k = 2, 4, 5, 6, 19, 20, 23, 24, 35, 36, 37, 45, 53, 54, 55, 56, 59, 62, 63$ *have one polycycle.*

(e) *The phase portraits* pp_k *for* $k = 3, 52, 60$ *have two polycycles.*

(f) *The maximum number of separatrices of these phase portraits is* 26 *and it is reached in the phase portraits* pp_k *for* $k = 13, 14, 16, 22$, *and the minimum number of separatrices is* 9 *and it is reached in the phase portraits* pp_k *for* $k = 5, 19$.

(g) *The maximum number of canonical regions of these phase portraits is* 7 *and it is reached in the phase portraits* pp_k *for* $k = 13, 14, 16, 22, 23, 32, 36, 39, 40, 42, 44, 45, 48, 51, 57, 59, 61$, *and the minimum number of canonical regions is* 3 *and it is reached in the phase portraits* pp_k *for* $k = 5, 19, 58$.

The rest of the paper is dedicated to prove Theorem 1.

All quadratic systems admitting $y^2 - x^2(x+1) = 0$ as invariant curve can be written as systems (2) with the parameters $(a, b, c) \in \mathbb{R}^3 \setminus \{(0, 0, 0)\}$. We divide the study of the phase portraits of the differential system (2) in the parameter space $\mathbb{R}^3 \setminus \{(0, 0, 0)\}$ as follows:

Case 1: $a = 0$.
Subcase 1.1: $a = 0$ and $c = 0$. Then doing a convenient rescaling we can take $b = 1$.
Subcase 1.2: $a = 0$ and $c \neq 0$. Then doing a convenient rescaling we can take $c = 1$
Case 2: $a \neq 0$.
Subcase 2.1: $a \neq 0$, $c = 0$ and $b = 0$. Then doing a convenient rescaling we can take $a = 1$.
Subcase 2.2: $a \neq 0$, $c = 0$ and $b \neq 0$. Then doing a convenient rescaling we can take $b = 1$.
Subcase 2.3: $a \neq 0$ and $c \neq 0$. Then doing a convenient rescaling we can take $c = 1$.

In Section 2 we study the phase portraits in the Poincaré disc of the subcases 1.1, 1.2, 2.1 and 2.2. In Section 3 we study the phase portraits of subcase 2.3. In Section 4 we prove Theorem 1. Finally, in Section 5 there are two appendixes one dedicated in the Poincaré compactification and the other one to the separatrix configuration.

2. Phase portraits of the subcases 1.1, 1.2, 2.1 and 2.2

Now we start the analysis of these cases and subcases.

Case 1: $a = 0$.

Subcase 1.1: $a = 0$ and $c = 0$. Then $b \neq 0$ otherwise the system is not quadratic, and without loss of generality we can consider $b = 1$. Then system (2) becomes

$$\dot{x} = y(1 + 3x), \quad \dot{y} = \frac{1}{2}\left(2x + 9y^2\right), \tag{3}$$

and has the rational first integral

$$H(x, y) = \frac{27\,y^2 + 9\,x + 1}{(3\,x + 1)^3}.$$

System (3) has the three invariant algebraic curves: $f_2 = 0$, $g_1 = 3x + 1 = 0$ and $g_3 = 27\,y^2 + 9\,x + 1$. Additionally, has the three finite singular points $P_0(0,\,0)$, $P_-\left(-1/3,\,-\sqrt{6}/9\right)$ and $P_+\left(-1/3,\,\sqrt{6}/9\right)$. P_0 is a saddle, P_- is an unstable node and P_+ is a stable node.

In what follows we use the notation introduced in the Appendix for studying the infinite singular points using the Poincaré compactification. The origin of the chart (U_1, F_1) is a nilpotent singular point and using Theorem 3.5 of [Dumortier *et al.*, 2006] is a saddle, and doing blows ups we get its local phase portrait as it shows in Figure 2. Moreover, the origin of the local chart U_2 is a hyperbolic stable node. The local and the global phase portraits of system (3) are given in Figure 2.
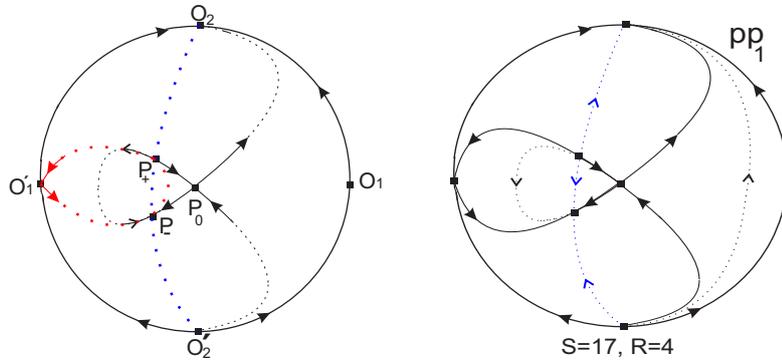

Fig. 2: The local and the global phase portraits of system (3). Here $a = c = 0$, $b = 1$ in system (2).

Subcase 1.2: $a = 0$ and $c \neq 0$. Without loss of generality we can consider $c = 1$, and system (2) can be written as

$$\begin{aligned}
\dot{x} &= by + (3b - 2)xy, \\
\dot{y} &= bx + x^2 + \left(\frac{9}{2}b - 3\right)y^2,
\end{aligned} \tag{4}$$

where this b is the old b/c. For $b = 2/3$ system (4) is a Hamiltonian system with the first integral $H = x^3 + x^2 - y^2$. System (4) for $b \neq 2/3$ has the rational first integral

$$H(x, y) = \frac{b^3 + 3\,b^2\,(3\,b - 2)\,x + 2\,\left(9\,b^2 - 12\,b + 4\right)x^2 + \left(27\,b^3 - 54\,b^2 + 36\,b - 8\right)y^2}{(3\,bx + b - 2\,x)^3}.$$

The curve $g_2 = b^3 + 3b^2(3b-2)x + 2(9b^2 - 12b + 4)x^2 + (27b^3 - 54b^2 + 36b - 8)y^2 = 0$ is a conic for $b \neq 2/3$ and it is classified as follows: For $b \in (-\infty, 0) \cup (0, 2/3)$ is a hyperbola, for $b \in (2/3, 8/9)$ an imaginary ellipse, and for $b > 8/9$ is a real ellipse. For $b = 0$ we obtain two real invariant straight lines that intersect into a point. For $b = 8/9$ the conic is formed by two parallel imaginary straight lines.

System (4) has the finite singular points (whenever they exist, see also Table 1)

$$P_0(0,0), \; P_1(-b, 0), \; P_-\left(\frac{b}{2-3b}, -\frac{b\sqrt{2b-2}}{(3b-2)^{3/2}}\right), \; P_+\left(\frac{b}{2-3b}, \frac{b\sqrt{2b-2}}{(3b-2)^{3/2}}\right).$$

Note that the points P_- and P_+ are the intersection points of the three curves $f_2 = 0$, $g_2 = 0$ and $g_1 = (3b-2)x + b = 0$.

For $b \in (0, 2/3) \cup (1, \infty)$ the point P_1 is on the left hand side of the straight line passing through the points P_- and P_+. For $b \in (-\infty, 0) \cup (0, 2/3) \cup (1, +\infty)$ the points $P_\pm$ exist. For $b = 0$ the four points collide into P_0. For $b = 1$ the three points P_+, P_- and P_1 collide between them. For $2/3 \leq b < 1$ only exist the finite singular points P_0 and P_1.

The point P_0 has the Jacobian matrix

$$\begin{pmatrix} 0 & b \\ b & 0 \end{pmatrix},$$

and its eigenvalues are $\pm b$. For $b = 0$ the point P_0 is linearly zero and doing blow–ups we obtain that its local phase portrait is the union of two elliptic and two parabolic sectors, see Figure 4.

The point P_1 has the Jacobian matrix

$$\begin{pmatrix} 0 & -3b^2 + 3b \\ -b & 0 \end{pmatrix},$$

and its eigenvalues are $\pm b\sqrt{3b-3}$. For $b = 0$ the point P_1 coincides with P_0. For $b = 1$ the point P_1 is a nilpotent point and by Theorem 3.5 of [Dumortier et $al.$, 2006] we have that P_1 is the union of one elliptic and one hyperbolic sectors separated by two parabolic sectors, see Figure 7.

The eigenvalues of the point P_+ are

$$\lambda_1 = \frac{\left(6\sqrt{2b-2}b + \sqrt{2}\sqrt{(b-1)(3b-2)^2} - 4\sqrt{2b-2}\right)b}{(3b-2)^{3/2}},$$

$$\lambda_2 = -\frac{b\left((-6b+4)\sqrt{2b-2} + \sqrt{2}\sqrt{(b-1)(3b-2)^2}\right)}{(3b-2)^{3/2}}.$$

The eigenvalues of the point P_- are

$$\lambda_1 = \frac{\left(-6\sqrt{2b-2}b + \sqrt{2}\sqrt{(b-1)(3b-2)^2} + 4\sqrt{2b-2}\right)b}{(3b-2)^{3/2}},$$

$$\lambda_2 = -\frac{\left(6\sqrt{2b-2}b + \sqrt{2}\sqrt{(b-1)(3b-2)^2} - 4\sqrt{2b-2}\right)b}{(3b-2)^{3/2}}.$$

For both points $P_\pm$ the product of its eigenvalues is $6b^2(b-1)/(3b-2)$.

In the chart (U_1, F_1) for $b < 2/3$ we obtain the infinite singular points

$$Q_+\left(\sqrt{\frac{2}{2-3b}}, 0\right), \quad Q_-\left(-\sqrt{\frac{2}{2-3b}}, 0\right).$$

The eigenvalues of the points $Q_\pm$ are $\pm\sqrt{4-6b}$.

b	$-\infty$		0		$2/3$		$8/9$		1		∞
P_0		S	pep	ep	S	S	S	S	S	S	S
P_1		C	$-$		C	C	C	C	C	$peph$	S
P_+		N^s	$-$		N^s	$-$	$-$	$-$	$-$	$-$	N^u
P_-		N^u	$-$		N^u	$-$	$-$	$-$	$-$	$-$	N^s
Q_-		S	S		S	$-$	$-$	$-$	$-$	$-$	$-$
Q_+		S	S		S	$-$	$-$	$-$	$-$	$-$	$-$
O_2		N^u	N^u		N^u	N^s	N^s	N^s	N^s	N^s	N^s

Table 1: The finite singular points of system (4).

The singular point at the origin of the chart (U_2, F_2) has the Jacobian matrix

$$\begin{pmatrix} 1 - 3b/2 & b \\ 0 & 3 - 9b/2 \end{pmatrix},$$

and its eigenvalues are

$$\lambda_1 = 1 - 3/2\,b, \quad \lambda_2 = 3 - 9/2\,b.$$

Thus, for $b \neq 2/3$ it is a node, whereas for $b = 2/3$ it is a nilpotent singular point, and by Theorem 3.5 of [Dumortier *et al.*, 2006] it is a stable node.
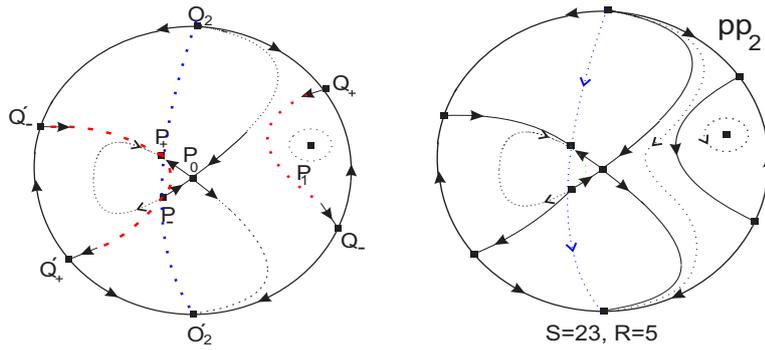
Fig. 3: The local and the global phase portraits of system (4). Here $a = 0$, $b < 0$ and $c = 1$. The curve $g_2 = 0$ is a hyperbola.
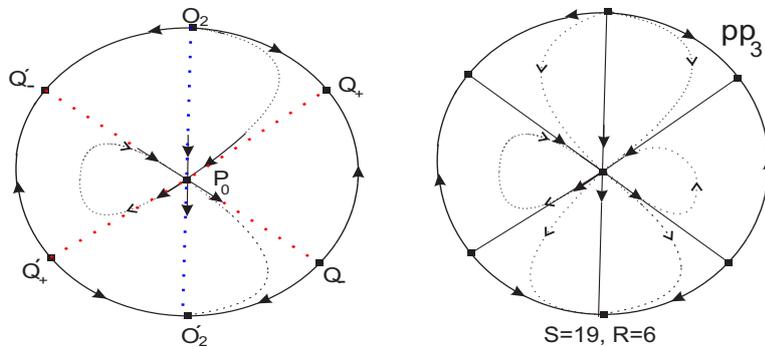
Fig. 4: The local and the global phase portraits of system (4). Here $a = b = 0$ and $c = 1$. The curve $g_2 = 0$ are two intersecting real lines.
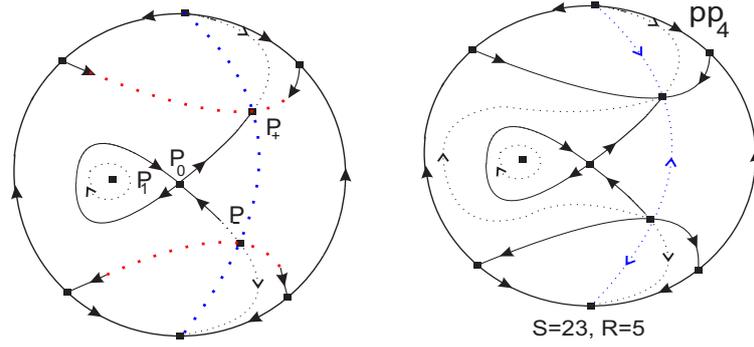
Fig. 5: The local and the global phase portraits of system (4). Here $a = 0$, $b \in (0, 2/3)$ and $c = 1$. The curve $g_2 = 0$ is a hyperbola.
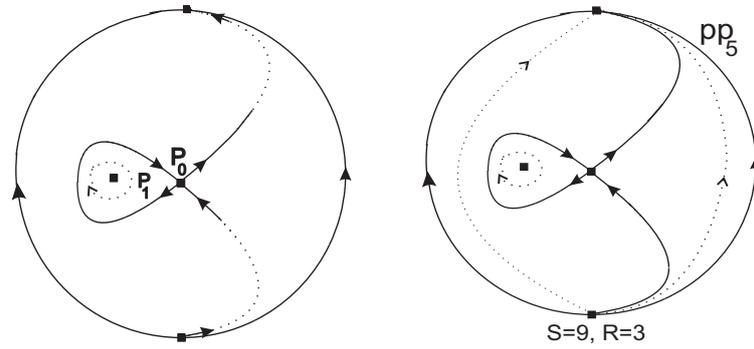

Fig. 6: The local and the global phase portraits of system (4). Here $a = 0$, $b \in [2/3, 1)$ and $c = 1$. For $b = 2/3$ the system is Hamiltonian with $H(x, y) = -x^3 - x^2 + y^2$ and admits the exponential factor $F = e^x$. For $b \in (2/3, 8/9)$ the curve $g_2 = 0$ is an imaginary ellipse whereas for $b = 8/9$ are two parallel imaginary straight lines. For $b \in (8/9, 1)$ the curve $g_2 = 0$ is a real ellipse.
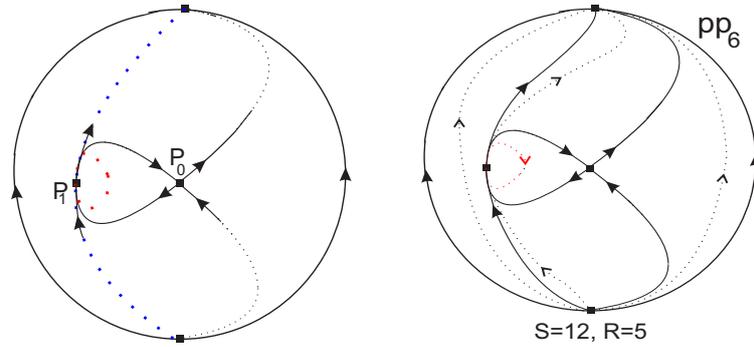
Fig. 7: The local and the global phase portraits of system (4). Here $a = 0$, $b = c = 1$. The curve $g_2 = 0$ is a real ellipse.

We note that the family (2) is invariant under the symmetry

$$(x, y, a, t) \rightarrow (x, -y, -a, -t). \tag{5}$$

Due to this symmetry when $a = 0$ the phase portraits of the differential system (2) is symmetric with respect to the x-axis, all the phase portraits of the quadratic polynomial differential systems having a symmetry with respect to a straight line have been classsified in [Llibre & Medrado, 2005], but in this paper are not described whose of these phase portraits have the invariant algebraic curve $f_2 = 0$.

In the paper [Llibre et $al.$, 2021] are classified the phase portraits of all the quadratic polynomial
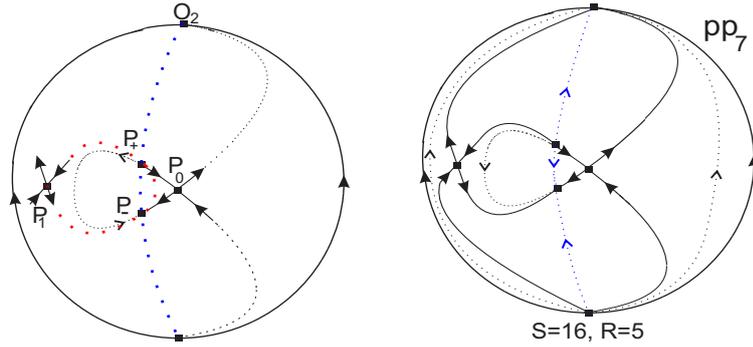
Fig. 8: The local and the global phase portraits of system (4). Here $a = 0$, $b > 1$ and $c = 1$. The curve $g_2 = 0$ is a real ellipse.

differential systems having an invariant algebraic curve of degree 3 and a Darboux invariant. Under these assumptions the invariant algebraic curve of degree 3 when it is irreducible is homeomorphic to the cubic $f_1 = 0$. So any of the phase portraits studied in this paper can appear in the paper [Llibre *et al.*, 2021].

Case 2: $a \neq 0$. Due to the symmetry (5) without loss of generality we can restrict our study to $a > 0$. We distinguish the following cases.

Subcase 2.1: $a \neq 0$ and $c = b = 0$. Then system (2) becomes

$$\dot{x} = ax(x + 1), \qquad \dot{y} = \frac{1}{2}ay(2 + 3x), \tag{6}$$

and it has the rational first integral $H = x^2(x + 1)/y^2$. Without loss of generality we can consider that $a = 1$. The unique finite singular points are $P_0 = (0, 0)$ and $P = (-1, 0)$. The point P_0 is an unstable node. The point $P \in \{f_2 = 0\}$ is a stable node. The origin O_2 of the chart (U_2, F_2) has a Jacobian matrix identically zero. Doing blow ups O_2 is the union of one parabolic and one hyperbolic sector. The local and the global phase portrait of system (6) is given in Figure 9.
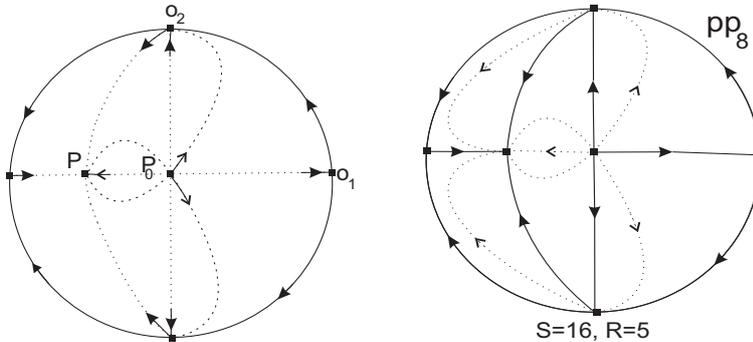

Fig. 9: The local and the global phase portraits of system (6). Here $a = 1$ and $b = c = 0$.

Subcase 2.2: $a \neq 0$ and $c = 0, b \neq 0$. Since $b \neq 0$ without loss of generality we can assume that $b = 1$. System (2) can be written as

$$\dot{x} = ax + y + ax^2 + 3xy, \qquad \dot{y} = x + ay + \frac{3}{2}axy + \frac{9}{2}y^2, \tag{7}$$

where now a is the previous a/b.

System (7) has three finite singular points:

$$P_0 = (0, 0), \qquad P_\pm = \left(-\frac{1}{3} + \frac{1}{18}a^2 \pm \frac{1}{18}A, \quad \frac{1}{54}\frac{-9a^2 \pm 3A - a^4 \mp a^2A}{a} \right),$$

with $A = a\sqrt{24 + a^2}$. Note that $P_0, P_\pm$ are points of the curve $f_2 = 0$. For $a = 1$ the point P_+ collides with P_0. The point P_- is always on the left hand side of the point P_+. For $a > \sqrt{3}$ the point P_- is upper the point P_+, here left hand side or upper are with respect to the x and y axes.

The linear part at the origin P_0 has eigenvalues $a + 1$ and $a - 1$. So, for $a \in (0, 1)$ the origin P_0 is a saddle. For $a > 1$ it is an unstable node. For $a = 1$ we have that P_0 is semi–hyperbolic and using Theorem 2.19 of [Dumortier *et al.*, 2006] we obtain that is a saddle–node.

Now we set

$$B_- = a^2 \left(a^6 - a^4 A + 30\,a^4 - 18\,a^2 A + 378\,a^2 + 1728 - 72\,A\right),$$

and note that for $a > 0$ we have that $B_- > 0$. At the point P_- the eigenvalues are

$$\lambda_{1,2} = \frac{1}{72} \frac{-24\,A - 42\,a^2 - a^4 + a^2 A \pm \sqrt{2B_-}}{a} < 0,$$

and consequently that P_- is a stable node.

We additionally set

$$B_+ = a^2 \left(a^6 + 30\,a^4 + a^4 A + 378\,a^2 + 18\,a^2 A + 1728 + 72\,A\right),$$

and for $a > 0$ we have that $B_+ > 0$. The eigenvalues associated to the point P_+ are

$$\lambda_{1,2} = -\frac{1}{72} \frac{42\,a^2 + a^4 + a^2 A - 24\,A \pm \sqrt{2B_+}}{a}.$$

We have that $\lambda_1 > 0$ and $\lambda_2 > 0$ if $a \in (0, 1)$, and $\lambda_1 \lambda_2 < 0$ if $a > 1$. So for $a \in (0, 1)$ the point P_+ is an unstable node and for $a > 1$ is a saddle.

In the chart (U_1, F_1) we obtain the two infinite singular points $O_1(0, 0)$ and $Q(-1/3, 0)$. The origin O_1 is a saddle, and the point Q_+ has eigenvalues 0 and $-a/2$, so it is semi-hyperbolic. By Theorem 2.19 of [Dumortier *et al.*, 2006] we obtain that the point Q is a saddle–node. The origin of the chart (U_2, F_2) is a stable node.

The local and the global phase portraits of system (6) are given in Figures 10, 11, 12 and 13.
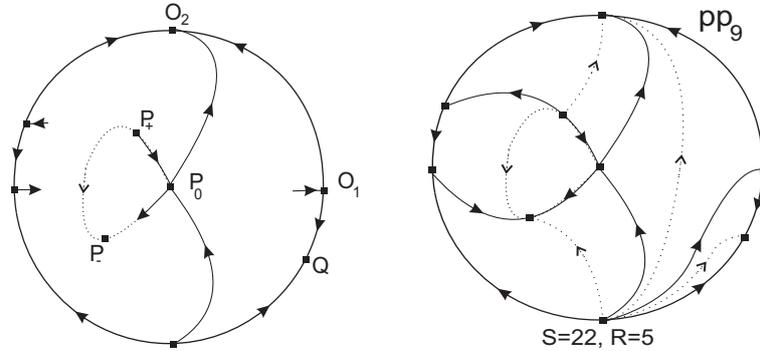

Fig. 10: The local and the global phase portraits of system (6). Here $c = 0$, $b = 1$ and $a \in (0, 1) \cup (1, \sqrt{3})$.

For $a = 1$ system (7) has only two singular points. The origin has eigenvalues $0, 2$ and using Theorem 2.19 of [Dumortier *et al.*, 2006] it is a saddle–node. The singular point $(-5/9,\ -10/27)$ is a stable node and is on the curve $f_2 = 0$, see Figure 11.

3. Phase Portraits of the subcase 2.3

Subcase 2.3: $a \neq 0$ and $c \neq 0$. Without loss of generality we can consider $c = 1$. System (2) becomes

$$\begin{aligned}
\dot{x} &= ax + by + ax^2 + (3b - 2)xy, \\
\dot{y} &= bx + ay + x^2 + \frac{3}{2}axy + \left(\frac{9}{2}b - 3\right)y^2.
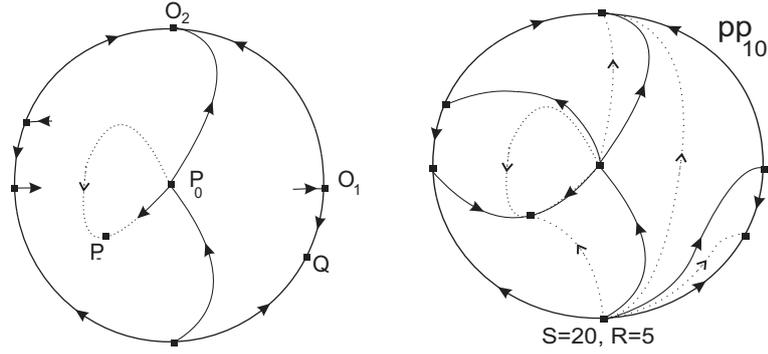\end{aligned} \tag{8}$$

Fig. 11: The local and the global phase portraits of system (6). Here $c = 0$, $a = b = 1$.

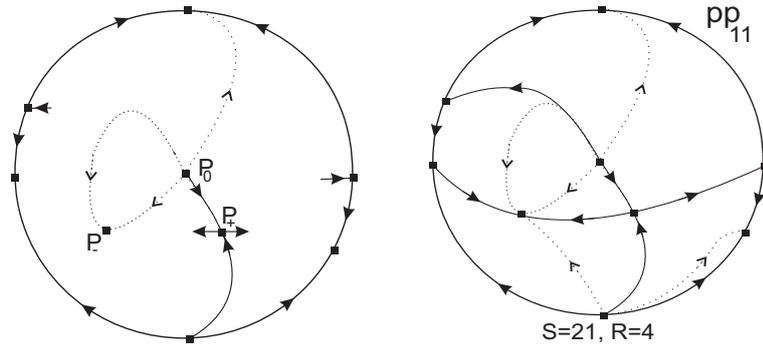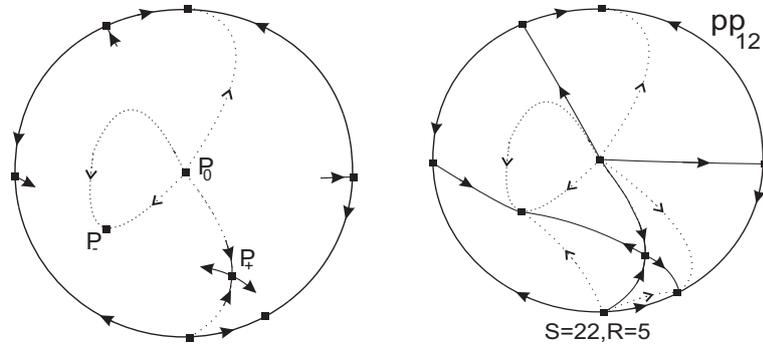Fig. 12: The local and the global phase portraits of system (6). Here $c = 0$, $b = 1$ and $a = \sqrt{3}$.

Fig. 13: The local and the global phase portraits of system (6). Here $c = 0$, $b = 1$ and $a > \sqrt{3}$.

System (8) has the following finite singular points (whenever are defined):

$$P_0 = (0,0), \qquad P_1 = \left(-b, \frac{a}{3}\right), \qquad P_\pm = (x_0, y_0),$$

with

$$x_0 = \frac{a^2 - 6b^2 + 4b \pm a\sqrt{24b^2 - 40b + a^2 + 16}}{2(3b-2)^2},$$

$$y_0 = \frac{-9ab^2 + 18ab - a^3 - 8a \pm (3b^2 - a^2 - 2b)\sqrt{24b^2 - 40b + a^2 + 16}}{2(3b-2)^3}.$$

In the chart (U_1, F_1) system (8) has the infinite singular points (whenever they exist)

$$Q_{\mp} = \left(\frac{-a \pm \sqrt{a^2 - 24b + 16}}{2(3b - 2)}, \quad 0 \right).$$

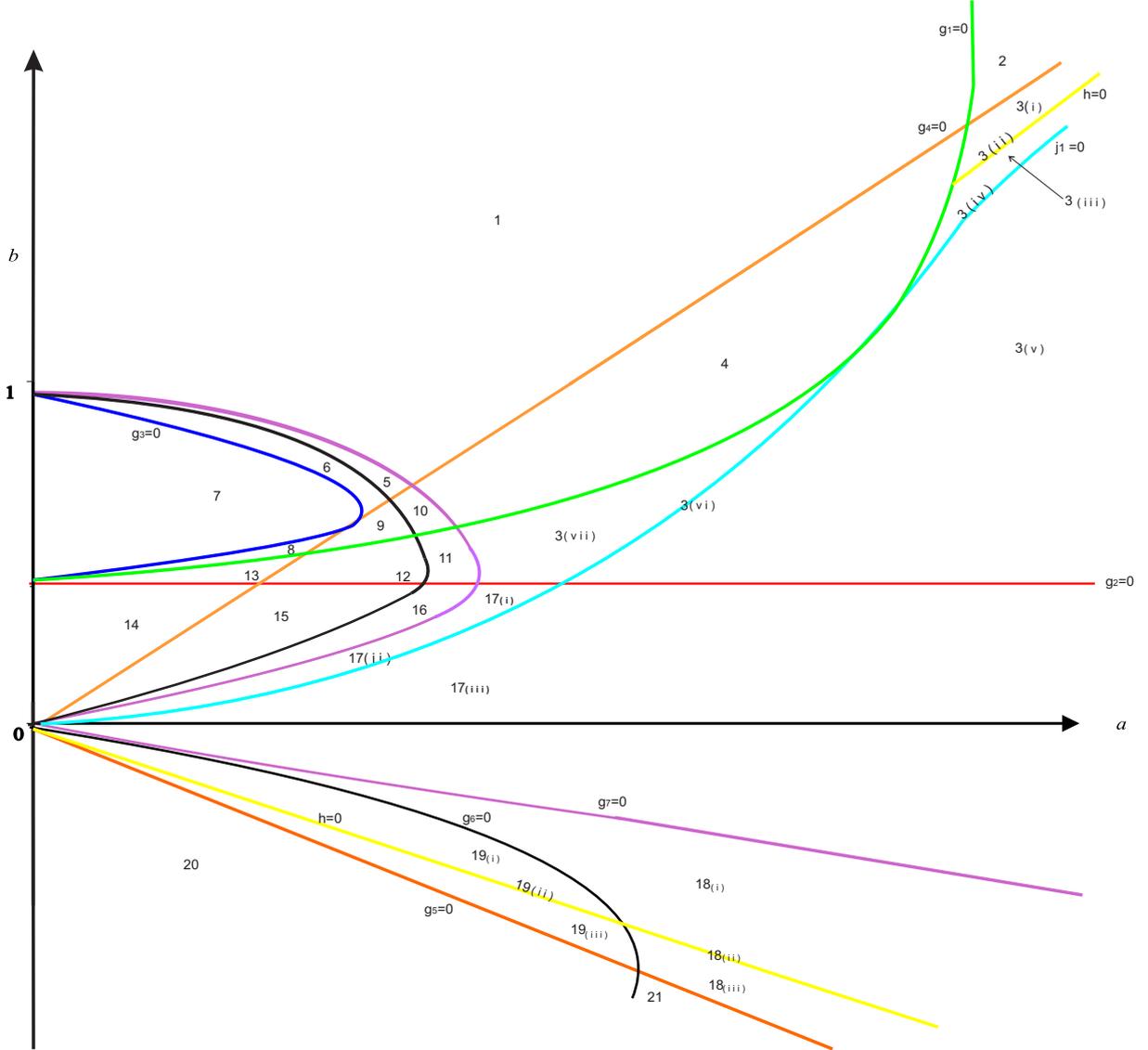The origin of the chart (U_2, F_2) is an infinite singular point of system (8).

Fig. 14: The bifurcation curves define 21 regions for system (8) with $a \neq 0$ and $c \neq 0$, i.e. $c = 1$ withought loss of generality.

We define the following bifurcations curves

$$
\begin{aligned}
&g_1 = a^2 + 16 - 24b, &&g_5 = a + b = 0, \\
&g_2 = 3b - 2 = 0, &&g_6 = 9a^2b^2 - 24a^2b + 64a^2 - 432b^2 + 432b^3 = 0, \\
&g_3 = 24b^2 - 40b + a^2 + 16 = 0, \quad &&g_7 = a^2 + 9b^3 - 9b^2. \\
&g_4 = a - b = 0,
\end{aligned}
$$

We also consider the curves

$$h = a^2 + \sqrt{g_1}\, a - 6b^2 + 4b, \qquad j_1 = b - \frac{1}{3}a. \tag{9}$$
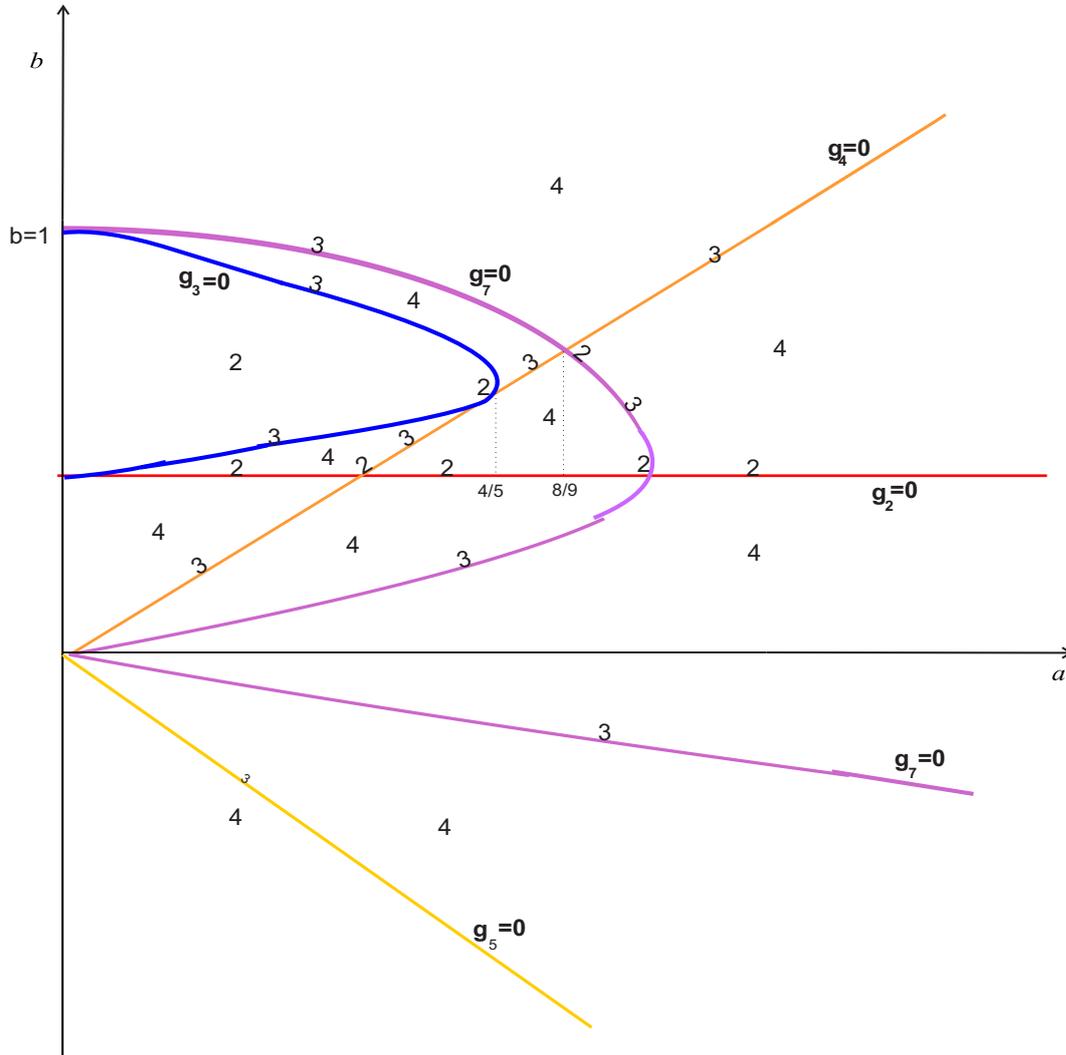
3.1. *Finite Singular Points*

Fig. 15: The number of finite singular points of system (8) in the different regions, lines and points.

Lemma 1. *The number of finite singular points of system* (8) *is given in Figure* 15.

Proof. Note that the points $P_\pm$ are not defined whenever $g_2 = 0$ and also when $g_3 < 0$. Addicionally, on $g_3 = 0$ the two points $P_\pm$ collide between them. Moreover, on the curve $g_7 = 0$ for $b \in (-\infty, 0)$ the point P_1 collide with the point P_+ and for $b \in (0, 1)$ the point P_1 collide with P_-. For $a = b = 8/9$ the point P_+ collide with P_0 whereas the point P_- collide with P_1. On the straight line $g_5 = 0$ the point P_+ colapse with P_0. On $g_4 = 0$ for $a = b > 4/5$ the point P_+ colapse with P_0, whereas for $0 < a = b < 4/5$ the point P_- colapse with P_0. Finally for $a = b = 4/5$ the points $P_\pm$ collide with the point P_0. ∎

Lemma 2. *The local phase portrait at the point P_0 is given in Figure* 16.

Proof. The point P_0 has eigenvalues $a \pm b$. Hence for $b > a$ or $b < -a$ we have that P_0 is a hyperbolic saddle. For $b > a$ or $b > -a$ the point P_0 is a hyperbolic unstable node. Over the straight lines $g_4 = 0$ and $g_5 = 0$ the point P_0 is a semi–hyperbolic singular point, and from Theorem 2.19 of [Dumortier *et al.*, 2006] we have that for $a \neq 4/5$ it is a saddle–node whereas for $a = 4/5$ it is a saddle. ∎
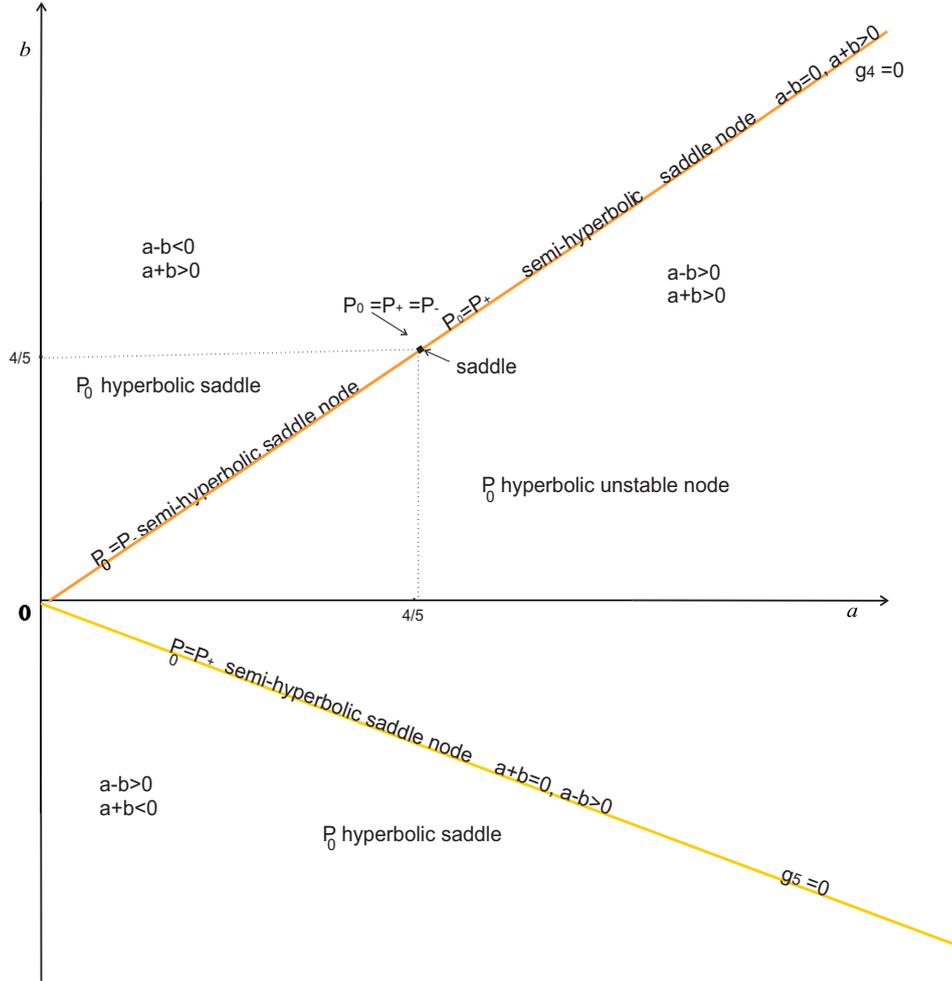
Fig. 16: The local phase portrait at the origin $P_0 = (0,0)$.

Remark 3.1. The finite singular points $P_\pm$ are always points of the invariant curve $f_2 = 0$. So cannot be foci or centers.

Lemma 3. *The local phase portrait at the point P_1 is given in Figure* 17.

Proof. The point P_1 has eigenvalues $e_\pm = ab/4 - a/3 \pm \sqrt{g_6}/12$. For $g_6 < 0$ the eigenvalues become comblex with non–zero real part. On $g_6 = 0$ we have that $e_+ = e_-$ and P_1 is a node and for $g_6 > 0$ we have two different real eigenvalues. Note that $e_- e_+ = -g_7/3$. Hence, for $g_7 > 0$ we have that P_1 is a hyperbolic saddle, whereas for $g_7 < 0$ and $g_6 > 0$ the point P_1 is a hyperbolic stable node. On $g_7 = 0$ one of the eigenvalues of P_1 becomes zero and P_1 is semi–hyperbolic, and from Theorem 2.19 of [Dumortier *et al.*, 2006] we have that P_1 is a saddle–node. ∎

Lemma 4. *The local phase portrait at the singular point P_+ is given in Figure* 18.

Proof. We recall that the point P_+ is defined for $g_2 \neq 0$ and $g_3 \geq 0$. On the curve $g_3 = 0$ the point P_+ coincides with P_-. For $a = b = 4/5 \in \{g_3 = 0\} \cap \{g_4 = 0\}$ the points P_+ and P_- collide with P_0. Additionally, the point P_+ has the eigenvalues

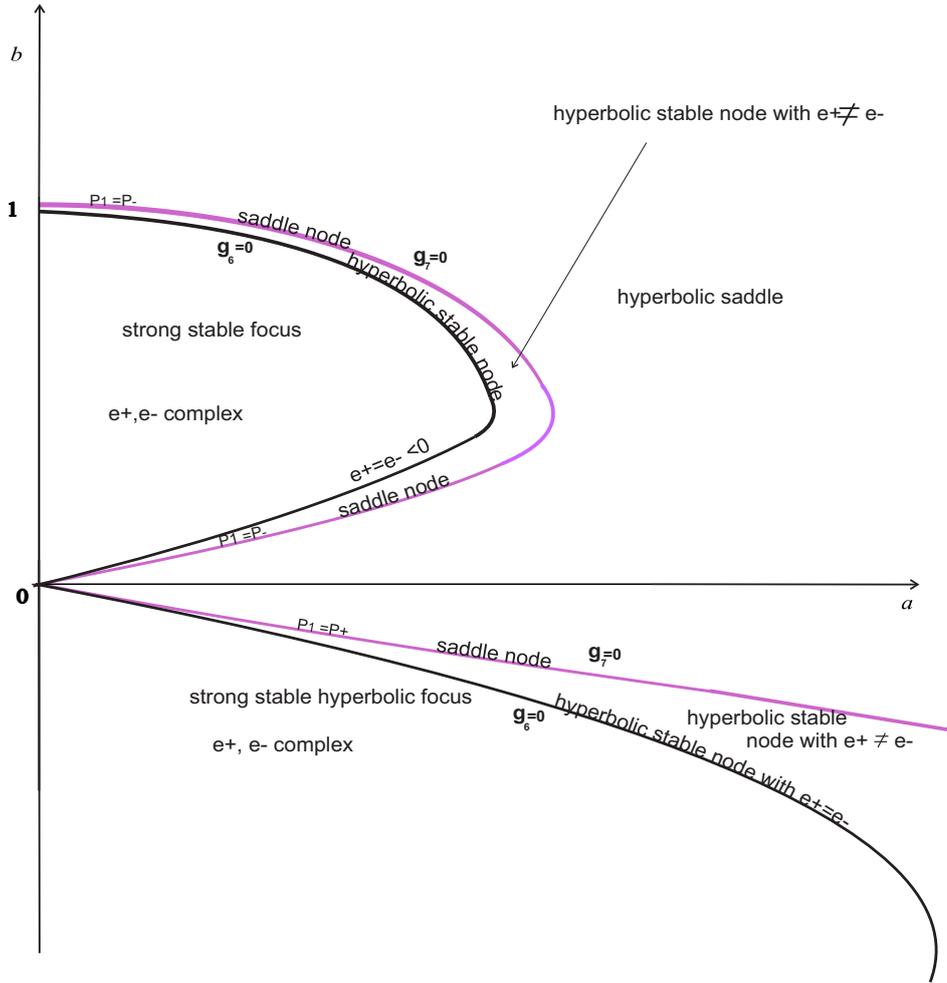$$\frac{a(-a^2 - 42\,b^2 + 76\,b - 32) + (-a^2 + 24\,b^2 - 16\,b)\,\sqrt{g_3} \pm \sqrt{2A_+}}{8\,(3\,b - 2)^2},$$

Fig. 17: The local phase portrait at the singular point $P_1 = (-b, a/3)$.

where

$$A_\pm = \left(\pm a^5 \pm 18a^3b^2 \pm 72ab^4 \mp 12a^3b \mp 96ab^3 \pm 32a\,b^2\right)\sqrt{g_3}$$
$$+a^6 + 30\,a^4b^2 + 378\,a^2b^4 + 1728\,b^6 - 32\,a^4b - 792\,a^2b^3 - 5184\,b^5 + 8\,a^4$$
$$+552\,a^2b^2 + 5760\,b^4 - 128\,a^2b - 2816\,b^3 + 512\,b^2.$$

We observe that both eigenvalues cannot be zero simultaneously. Note that $A_+ \geq 0$ due to Remark 3.1. The product of the eigenvalues det_+ is

$$det_+ = -\frac{a\left(45\,b^3 + 2\,a^2 - 78\,b^2 + 32\,b\right)\sqrt{g_3}}{4\left(3\,b - 2\right)^3} - \frac{g_3\left(-9\,b^3 + 2\,a^2 + 6\,b^2\right)}{4\left(3\,b - 2\right)^3}.$$

If $det_+ < 0$ then P_+ is a saddle, see Figure 18. Note that $det_+ = 0$ on $g_3 = 0$, $g_5 = 0$ and for $a = b > 4/5$ on $g_4 = 0$. For $b < 0$ on the points of the curve $g_7 = 0$ we have that $det_+ = 0$. In these cases we have that P_+ is a semi–hyperbolic singular point and so we apply Theorem 2.19 of [Dumortier *et al.*, 2006], see also Figure 18. If $det_+ > 0$ the point P_+ is a node, see Figure 18. ■

Lemma 5. *The local phase portrait at the point P_- is given in Figure* 19.

Proof. The point P_- is defined for $g_3 \geq 0$ and $g_2 \neq 0$, and has eigenvalues

$$\frac{a(-a^2 - 42\,b^2 + 76\,b - 32) + \left(a^2 - 24\,b^2 + 16\,b\right)\sqrt{g_3} \pm \sqrt{2A_-}}{8\left(3\,b - 2\right)^2},$$
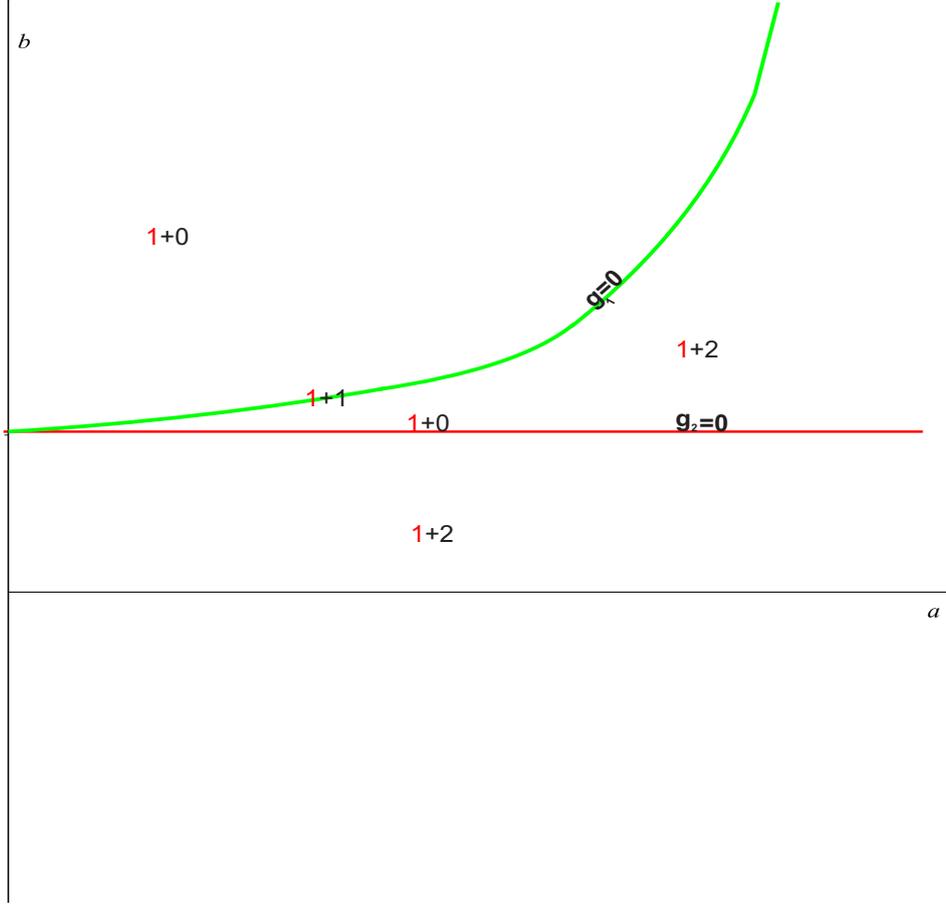
Fig. 18: The local phase portrait at the singular point P_+.

where A_- is defined in Lemma 4.

Note that for all the values of the parameters we have that $A_- \geq 0$, see also Remark 3.1. The product of the eigenvalues det_- is

$$det_- = \frac{a\left(45\,b^3 + 2\,a^2 - 78\,b^2 + 32\,b\right)\sqrt{g_3}}{4\left(3\,b-2\right)^3} - \frac{g_3\left(-9\,b^3 + 2\,a^2 + 6\,b^2\right)}{4\left(3\,b-2\right)^3}.$$

If $det_- < 0$ the point P_- is a saddle, see Figure 19. For $g_3 = 0$ we have that $det_- = 0$. Additionally, for $b > 0$ on the points of $g_7 = 0$ we have that $det_- = 0$. For $b > 4/5$ and additionally $g_4 = 0$ we also have $det_- = 0$. In these cases the point P_- is semi–hyperbolic and so we apply Theorem 2.19 of [Dumortier *et al.*, 2006], see Figure 19. If $det_- > 0$ the point P_- is a node, see Figure 19. ∎

3.2. *Infinite singular points*

Lemma 6. *The number of infinite singular points of system* (8) *is given in Figure* 20.

Proof. In the local chart (U_1, F_1) system (8) becomes

$$\dot{z}_1 = 1 + bz_2 + \frac{1}{2}\,az_1 + \left(\frac{3}{2}\,b - 1\right)z_1{}^2 - bz_1{}^2z_2,$$
$$\dot{z}_2 = -z_2\left(az_2 + bz_1\,z_2 + a + 3\,bz_1 - 2\,z_1\,c\right),$$

Fig. 19: The local phase portrait at the singular point P_-.

and for $g_1 \geq 0$ and $g_2 \neq 0$ it has the infinite singular points

$$Q_\pm = \left(\frac{-a \pm \sqrt{g_1}}{2g_2}, \quad 0 \right).$$

Note that neither Q_- nor Q_+ coincide with the origin of the chart (U_1, F_1). The two points $Q_\pm$ collided between them over the curve $g_1 = 0$.

In the local chart (U_2, F_2) system (8) becomes

$$\dot{z}_1 = bz_2 + \left(-\frac{3}{2} b + 1 \right) z_1 - \frac{1}{2} a z_1{}^2 - b z_1{}^2 z_2 - z_1{}^3,$$

$$\dot{z}_2 = -\frac{1}{2} z_2 \left(2 b z_1 z_2 + 2 a z_2 + 2 z_1{}^2 + 3 a z_1 + 9 b - 6 \right),$$

and the origin of the local chart (U_2, F_2) is an infinite singular point. ∎

Lemma 7. *The stability of the infinite singular points of system* (8) *in the local chart* (U_1, F_1) *is given in Figure* 21.

Proof.

Fig. 20: The number of the infinite singular points of system (8).

We recall that the points $Q_\pm$ are not defined on $g_2 = 0$. For $g_1 < 0$ are not real points, so we will consider them only when $g_1 \geq 0$. The point Q_+ has eigenvalues

$$\frac{-a \pm \sqrt{5\,a^2 + 4\,a\sqrt{g_1} - 96\,b + 64}}{4}.$$

Note that on $g_1 = 0$ the point Q_+ collide with Q_- and is a semi–hyperbolic saddle–node. Also note that both eigenvalues at the point Q_+ cannot be zero. The product of the eigenvalues is

$$Det_+ = -1/4\,a^2 - 1/4\,a\sqrt{g_1} + 6\,b - 4,$$

and for $g_1 > 0$ we have that $Det_+ < 0$, and so the point Q_+ is a saddle. The point Q_- has eigenvalues

$$\frac{-a \pm \sqrt{5\,a^2 - 4\,a\sqrt{g_1} - 96\,b + 64}}{4},$$

and on $g_1 = 0$ is a semi–hyperbolic saddle–node. The product of the eigenvalues at the point Q_- is

$$Det_- = -1/4\,a^2 + 1/4\,a\sqrt{g_1} + 6\,b - 4.$$

The point Q_- changes from a saddle to a node when the values of the parameters of the system cross the line $g_2 = 0$, see Figure 21. ■

Lemma 8. *For $b < 2/3$ the origin of the local chart (U_2, F_2) is an unstable node. If $b > 2/3$ is a stable node. If $b = 2/3$ the origin is the union of an elliptic and a hyperbolic sector separated by two parabolic sectors.*
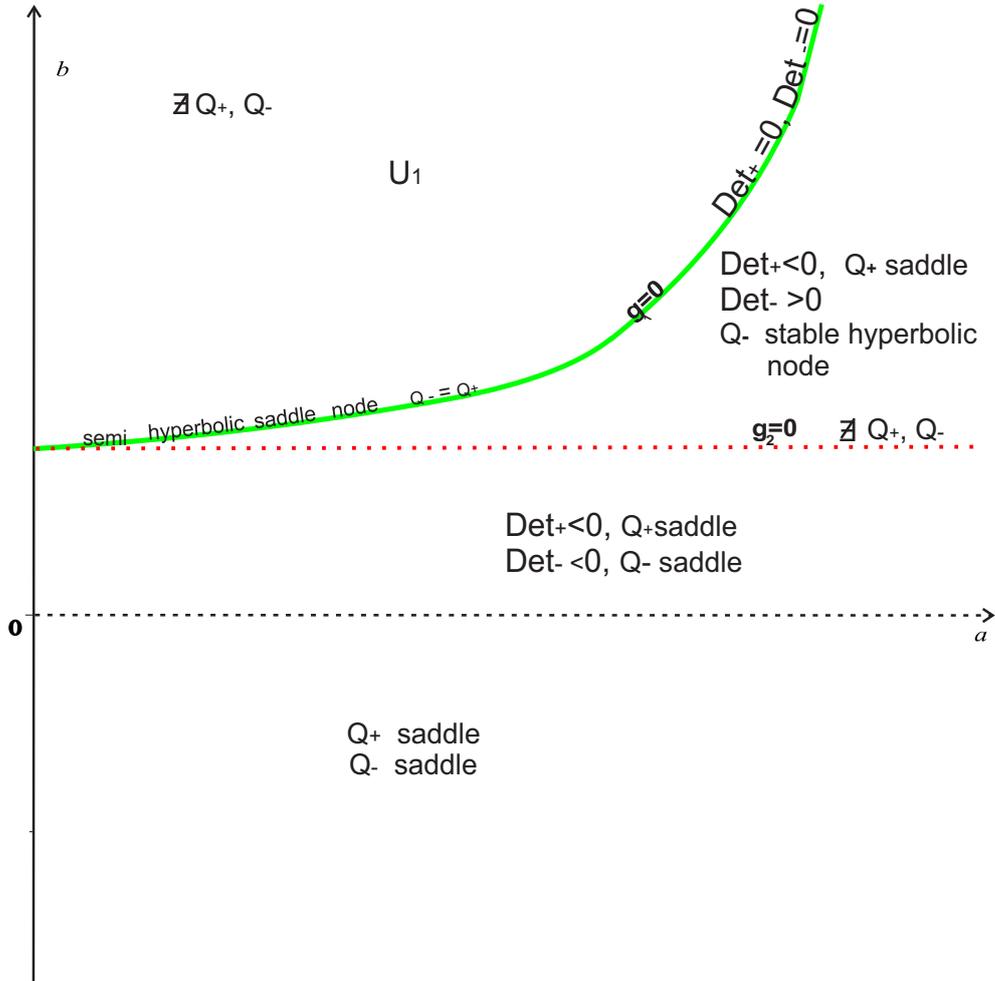
Fig. 21: The infinite singular points of the local chart (U_1, F_1).

Proof. The origin $O_2 = (0,0)$ of the chart (U_2, F_2) has the Jacobian matrix

$$\begin{pmatrix} -3/2\,b + 1 & b \\ 0 & 3 - 9/2\,b \end{pmatrix},$$

with eigenvalues $-3b/2 + 1$ and $3 - 9b/2$. For $b > 2/3$ the point O_2 is a stable hyperbolic node whereas for $b < 2/3$ becomes an unstable hyperbolic node. For $b = 2/3$ both eigenvalues become zero, (the Jacobian is not identically zero) so O_2 is a nilpotent singular point. Using Theorem 3.5 of [Dumortier *et al.*, 2006] and the blow up technique we obtain that the point O_2 is the union of an elliptic and a hyperbolic sector separated by two parabolic sectors. Note that the straight line of the infinity locally is contained in the two parabolic sectors. ∎

Proposition 2. *For $g_1 > 0$ we obtain two distinct infinite singular points Q_- and Q_+. On the curve $g_1 = 0$ the two points collided: $Q_- = Q_+$ and one eigenvalue of them becomes zero. For $g_1 < 0$ the two infinite singular points Q_- and Q_+ do not exist.*

On the curve $g_2 = 0$ the singular points $P_\pm$ and $Q_\pm$ do not exist. The point P_+ changes from a saddle to a node when the parameters of the system cross the line $g_2 = 0$. Q_- changes from a node to a saddle when the parameters of the system cross this line and at this line the origin of (U_2, F_2) is a nilpotent singular point, see Figure 21.

On the bifurcation curve $g_3 = 0$ the two finite singular points $P_\pm$ collided between them. On $g_3 = 0$ for $a = b = 4/5$ the points $P_\pm$ collide to P_0. For $g_3 < 0$ the points $P_\pm$ do not exist. For $g_3 > 0$ see Figures 18 and 19.

On the line $g_4 = 0$ the point P_0 for $a \neq 4/5$ is a semi–hyperbolic saddle–node, whereas for $a = 4/5$ is a saddle. For $a = b > 4/5$ the point P_+ colapse with P_0 whereas for $0 < a = b < 4/5$ the point P_- colapse with P_0. For $a = b = 4/5$ both points $P_\pm$ collide to P_0 and is a saddle. For $a = b \in (4/5, 8/9)$ the point P_- is a saddle whereas for $a = b > 8/9$ is a stable node. For $a = b > 4/5$ the point P_+ changes from a saddle to a node. For $b < 4/5$ the point P_- changes from a saddle to a node when the parameters of the system cross the line $g_4 = 0$, see Figures 15, 16, 18 and 19.

On the line $g_5 = 0$ the P_0 is a semi–hyperbolic saddle–node. The point P_+ colapse to P_0. The point P_+ changes from a saddle to a node when the parameters of the system cross this line, see Figures 16 and 18.

On the curve $g_6 = 0$ the point P_1 is a hyperbolic stable node. For $g_6 < 0$ we have that P_1 has complex eigenvalues and consequently is a strong stable focus. For $g_6 > 0$ we have that P_1 has real eigenvalues, see Figure 17.

On the curve $g_7 = 0$ the point P_- collided with P_1 when $b > 0$ whereas for $b < 0$ the point P_+ collide with P_1. Note that the product of the eigenvalues of P_1 is $g_7/(-3)$. On $g_7 = 0$ the point P_1 is a semi–hyperbolic saddle–node. P_1 changes from a saddle to a node when the parameters of the system cross this line. The point P_1 changes from a saddle to a node when the parameters of the system cross the line $g_7 = 0$, see Figure 17.

Proof. The proof of Proposition 2 follows directly from Lemmas 1, 2, 3, 4, 5, 6, 7 and 8. ∎

In this section we study the global phase portraits of system (8): We draw the local phase portrait of the finite and infinite singular points in the Poincaré disc, see for details on the Poincaré compactification the Appendix 5. Additionally we plot in the Poincaré disc the invariant algebraic curve $f_2 = 0$. Finally, we should present all the global phase portraits.

Let L be a straight line and let q be a point of L. We say that q is a *contact point* of the straight line L with a vector field X, if the vector $X(q)$ is parallel to L.

For quadratic systems the following two results are well known.

Lemma 9. *On any straight line which is not invariant the total number of singular points and contact points is two. If there are two such points, P_1 and P_2, then the orbits intersecting the line ∞P_1 cross in the same sense as the orbits intersecting the line $P_2 \infty$, and in the opposite sense the orbits $P_1 P_2$.*

For a proof of Lemma 9 see the lemma in page 296 of Coppel [Coppel, 1966].

Lemma 10. *On any non invariant straight line through a finite singular point P reaching the infinity in a pair of infinite singular points the orbits crossing the segment ∞P have opposite sense to the orbits crossing the segment $P \infty$.*

Lemma 10 is equivalent to Lemma 9 when one of the contacts points mentioned in Lemma 9 goes to infinity. For a proof of Lemma 10 see [Artés *et al.*, 1998].

Remark 3.2. In what follows when we apply Lemmas 9 or 10 we must check that the straight lines mentioned in these lemmas are not invariant. In case that there are invariant we shall state this fact explicitly.

The following theorem also appears in Coppel's paper [Coppel, 1966].

Theorem 2. *A singular point in the interior of a closed path of a quadratic system must be either a focus or a center.*

Here a *closed path* is an invariant curve of the quadratic system contained in $\mathbb{R}^2$ homeomorphic to a circle such that in its neighborhood contained in the bounded region limited by it the Poincaré return map is defined.

Remark 3.3. In fact the proof which appears in Coppel's paper [Coppel, 1966] also works when the closed path of the quadratic system has some piece at infinity. So Theorem 2 also holds for closed paths having some orbit at infinity.

Theorem 3. *Let X be a vector field of class $\mathcal{C}^1$ on an open set $\Delta \subseteq \mathbb{R}^2$. Consider γ a closed path of X such that the bounded region $\mathcal{R}$ limited by γ is contained in Δ. Then there exist a singular point of X in $\mathcal{R}$, inside the region limited by γ.*

The proof of Theorem 3 is the same as the proof of Theorem 1.31 of [Dumortier *et al.*, 2006].
The next result is due to Berlinskiĭ [Berlinski, 1960].

Theorem 4. *Suppose that a quadratic system has four singular points. If the quadrilateral with vertices at these points is convex then two opposite singular points are saddles and the other two are antisaddles (nodes, foci, or centers). But if the quadrilateral is not convex then, either the three exterior vertices are saddles and the interior vertex is an antisaddle, or the exterior vertices are antissaddles and the interior vertex is a saddle.*

Next we prove that system (8) has no limit cycles.

Lemma 11. *System (8) has no limit cycles.*

Proof. Consider system (8) and $X = (P, Q)$ the corresponding vector field. According to Theorem 2 a possible limit cycle can appears only surrounding a focus. Note that for system (8) we only have a focus in the interior of the loop of the curve $f_2 = 0$ for the values of the parameters in the regions $r_6, r_7, r_8, r_9, r_{12}, r_{13}, r_{14}, r_{15}$, and on the lines $L_4, L_5, L_6, L_7, L_{13}, L_{14}, L_{26}, L_{27}, L_{28}, L_{29}$. Also we have a focus on the right side of this curve for the values of the parameters in the regions r_{19} and r_{20} and on the line L_8. The divergence of the system $(Pf_2^{-4/3}, Qf_2^{-4/3})$ is

$$D = \frac{\partial(P\,f_2^{-4/3})}{\partial x} + \frac{\partial(Q\,f_2^{-4/3})}{\partial y} = -\frac{a\,(3\,x + 4)}{6\,(-x^3 - x^2 + y^2)^{4/3}} = -\frac{a\,(3\,x+4)}{6f_2^{4/3}}.$$

Note that the vertical straight line $3x + 4 = 0$ does not intersect the invariant curve $f_2 = 0$. Hence D does not change sign in the regions containing the focus. Hence, by the Bendixon–Dulac criterium (see Theorem 7.12 of [Dumortier *et al.*, 2006]) there are no periodic orbits in the mentioned regions and lines in the (a, b) parameter plane, and so there are no limit cycles. ∎

In what follows a *heteroclinic loop* is formed by two saddles P_1 and P_2 and two different separatrices connecting these saddles and forming a loop in such a way that at least in one of the two sides of the loop a Poincaré return map is defined. Let $\mu_i < 0 < \lambda_i$ be the eigenvalues of the saddles P_i for $i = 1, 2$. Set

$$k = \frac{\mu_1}{\lambda_1}\frac{\mu_2}{\lambda_2}.$$

If $k < 1$ then the loop in the region limited by it is unstable, and if $k > 1$ then the loop is stable, see Poincaré [Poincaré, 1928] (see Theorem XVII).
For regions r_{19}, r_{20} and the line L_8 we have the following result.

Lemma 12. *For the values of the parameters in the regions r_{19}, r_{20}, and on the line L_8 system (8) has no connection between the separatrices of the saddles $Q_\pm$.*

Proof. We assume that there is a connection between the separatrices of the saddles $Q_\pm$ of system (8) for the values of the parameters in the regions r_{19} and r_{20}. Then there is a heteroclinic loop containing a focus. Note that for the points $Q\pm$ (see also Lemma 7)

$$k = \left(\frac{-a - \sqrt{5\,a^2 + 4\,a\sqrt{g_1} - 96\,b + 64}}{-a + \sqrt{5\,a^2 + 4\,a\sqrt{g_1} - 96\,b + 64}}\right)\left(\frac{-a - \sqrt{5\,a^2 - 4\,a\sqrt{g_1} - 96\,b + 64}}{-a + \sqrt{5\,a^2 - 4\,a\sqrt{g_1} - 96\,b + 64}}\right) > 1.$$

Thus the heteroclinic loop is stable. Since the focus in the interior of the heteroclinic loop is also stable it must exist a cicle limit by the Poincaré–Bendixson Theorem (see for instance Corollary 1.30 of [Dumortier *et al.*, 2006]). But this is in contradiction with Lemma 11.

Now we consider the values of the parameters on the line L_8. If there is a connection between the separatrices of the points Q_1 and Q_2, then they form a heteroclinic loop that must contain the focus. Working in a similar way as in Lemma 12 for the saddles Q_1 and Q_2 we obtain

$$k = \frac{\left(-a + \sqrt{5a^2 - 4a\sqrt{d} + 96a + 64}\right)\left(-a + \sqrt{5a^2 + 4a\sqrt{d} + 96a + 64}\right)}{\left(-a - \sqrt{5a^2 - 4a\sqrt{d} + 96a + 64}\right)\left(-a - \sqrt{5a^2 + 4a\sqrt{d} + 96a + 64}\right)} > 1,$$

with $d = a^2 + 24a + 16$. Thus this heteroclinic loop is stable. Since the focus in the interior of the heteroclinic loop is also stable by the Poincaré–Bendixon Theorem it must exist a limit cycle. But this is in contradiction with Lemma 11. ∎

3.3. *Phase portraits in the regions*

The bifurcation curves define 21 regions, see Figure 14. Here we are going to present all the phase portraits of system (8) in the Poincaré disc for the values of the parameters in each one of the 21 regions.
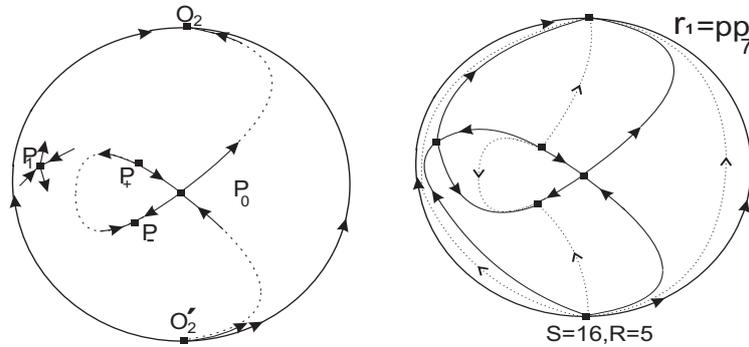
Fig. 22: The local and the global phase portraits of system (8) corresponding to the region r_1.

For the region r_1 we realize the following steps, see also Figure 22.

(i) According to Theorem 6 of the Appendix first we draw the separatrices in the Poincaré disc and then we should draw an orbit in each canonical region. This determines completely the global phase portraits in the Poincaré disc.

(ii) We first draw the local phase portrait of the finite and infinite singular points in the Poincaré disc, see Figure 22.

(iii) Next we study the $\alpha-$ and the $\omega-$limits of the separatrices.

(iv) Since in the region r_1 does not exist any focus we have that no limit cycle exist for the quadratic system (8), see Theorem 2.

(v) We should only study the separatrices of the point P_1 (saddle). The two unstable separatrices can only reach the infinite stable node O_2 or the finite stable node P_-. Additionally the $\omega-$limit of thess two unstable separatrices cannot be the same stable node, otherwise they should define a closed region and it should contain a stable separatrix without its $\alpha-$limit.

(vi) Finally, we obtain the unique global phase portrait in Figure 22.

Next we describe the phase portrait of system (8) corresponding to the values of the parameters in the region r_2, see Figure 23.

(i) In the finite region the stable separatrix of Q_+ can only have as $\alpha-$limit the unstable node O_2'.

(ii) By similar arguments as in the region r_1 we have that the two unstable separatrices of the point P_1 can only have as $\omega-$limit the points O_2 and P_-.

(iii) The unstable separatrix γ of the infinite point Q_+' in the finite region could have as $\omega-$limit the points P_-, P_1 or O_2. Consider the straight line passing on the points Q_+', P_- and Q_+. In the region r_2 the point
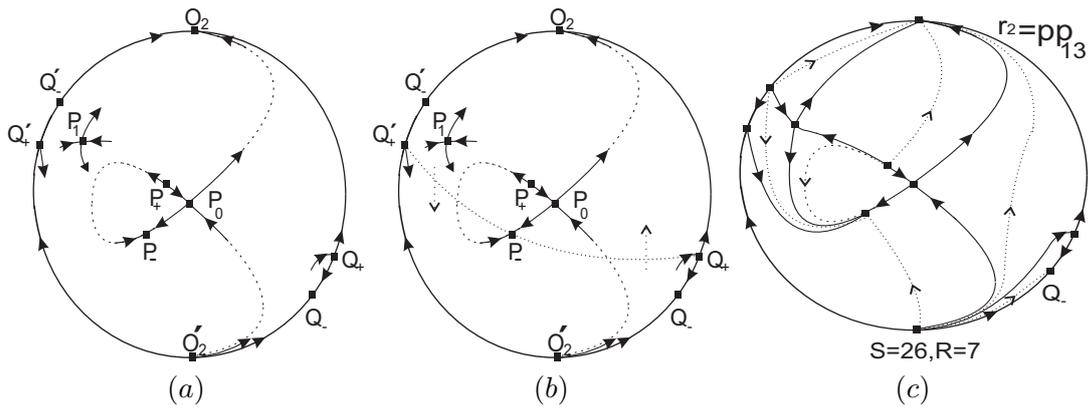
Fig. 23: The local and the global phase portraits of systems (8) corresponding to the region r_2.

P_1 is always upper this straight line. According to Lemma 10 the vector field have opposite direction in the two half–lines Q'_+P_- and P_-Q_+. Additionally note that P_1 is always at the same side of the straight line in the region r_2. Therefore the $\omega-$limit of γ must be the point P_-, see Figure 23(b).

(iv) The two stable separatrices of P_1 have the $\alpha-$limits at the points P_+ and Q'_-.

(v) Finally we obtain the unique global phase portrait in Figure 23(c).

In what follows we describe the phase portrait of system (8) corresponding to the region r_3, see Figure 24.

(i) Consider the straight line passing through the points Q_+, P_+ and Q'_+. We distinguish the following cases.

(i.1) The point P_- is below this straight line, see Figure 24(a). Then the direction of the loop on the curve $f_2 = 0$ determines the direction of the vector field on this line, see also Lemma 10. The separatrices of the points P_+, Q_+ and Q'_+ are as in Figure 24(a).

(i.2) For a and b satisfying the equation $h = 0$ (see (9)) the point P_- belong to this straight line and now the line is invariant for the vector field (8), see Figure 24(b).

(i.3) The point P_- is above this straight line. Then the direction of the vector field in the segment Q'_+P_+ is determined by the unstable node O'_2 see Figures 24(c),(d),(e_1), (e_2). Also note that the unstable separatrix of the saddle Q_+ must be upper this straight line, see also Lemma 10 (and also check the stable separatrix of the saddle Q'_+). For the same reason the unstable separatrices of the point P_+ must be as they are shown in Figures 24(c),(d),(e_1),(e_2).

Now consider the straight line L passing through the points Q_-, P_0 and Q'_-.

(j_1) The point P_1 can be upper this straight line L. Then, the unstable separatrices of P_1 can only have ω–limit the points O_2 and P_-. This determines the direction of the vector field over the straight line L, see Figures 24(a),(b),(c).

(j_2) For the values of the parameters a and b in the line 3(iv) (so a, b satisfying the equation $j_1 = 0$, see (9)) the point P_1 belong to the straight line L and so the line becomes invariant for the vector field (8), see Figure 24(d).

(j_3) The point P_1 can be below the straight line L. The unstable separatrices determine the direction of the vector field on this line, see Figure 24(e_1).

(ii) In all the cases the unstable separatrices of the point P_1 can have as $\omega-$ limit only the points O_2 and P_-.

(iii) In all the cases the stable separatrices of the point P_1 can only have as $\alpha-$ limit the points P_0 and Q'_-.

(iv) Now consider the straight line L' passing through the points Q_+, P_0 and Q'_+. In general, the point P_1 is above this straight line L'. So in general, in the finite region the unstable separatrix of the point Q'_+ must be bellow this straight line and therefore its ω-limit must be the point P_-. However, for the values of the parameters a and b in the line 3(vii) (so a, b satisfying the equation $j_1 = 0$, see (9)) the point P_1 belongs to this straight line L' and so becomes invariant, see Figure 24(e_2).

(v) The local phase portrait (a) yields to the global phase portrait (f). The local phase portrait (b) yields
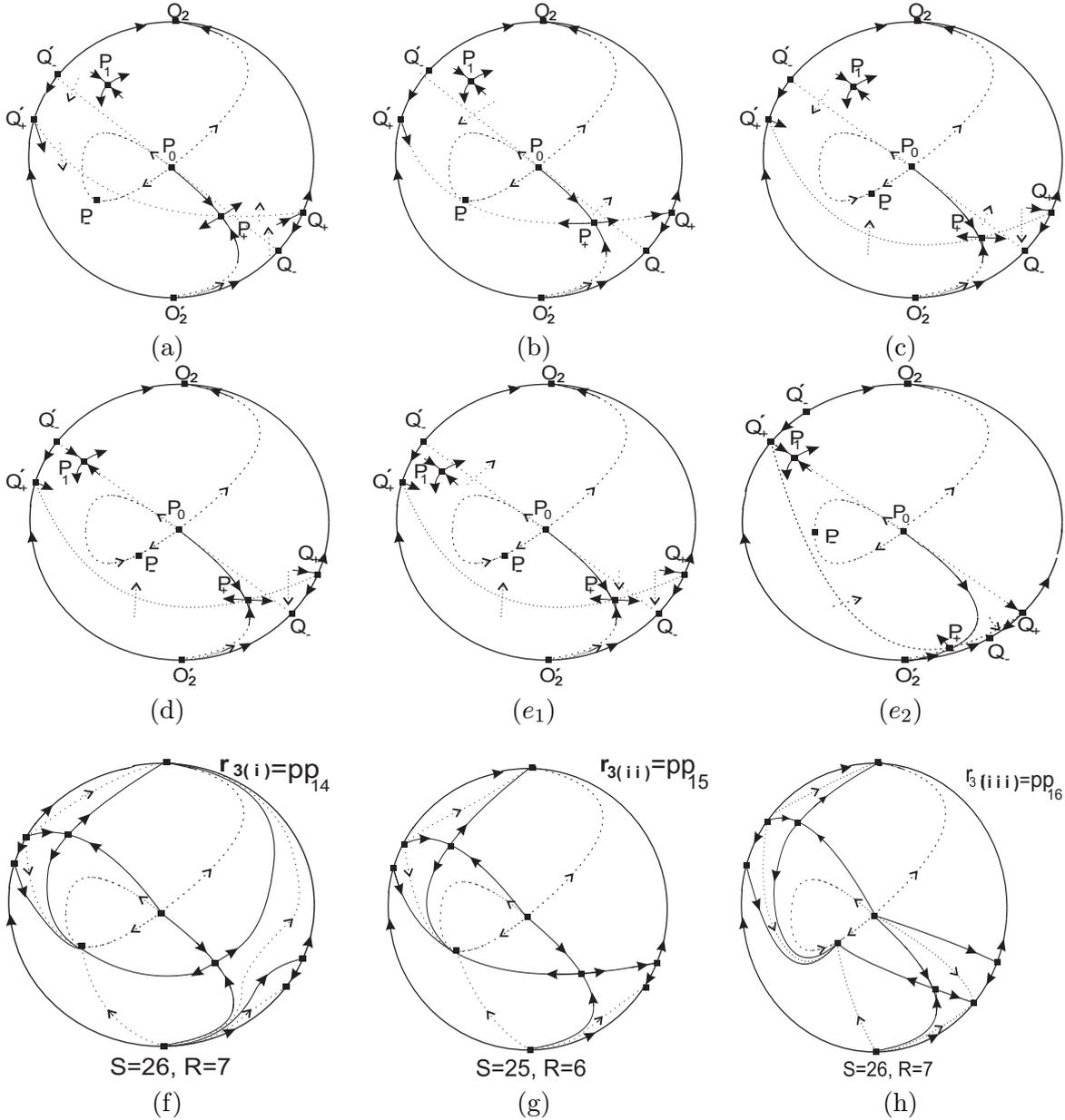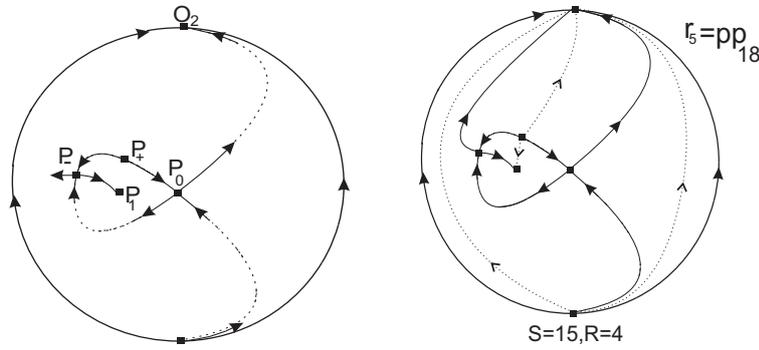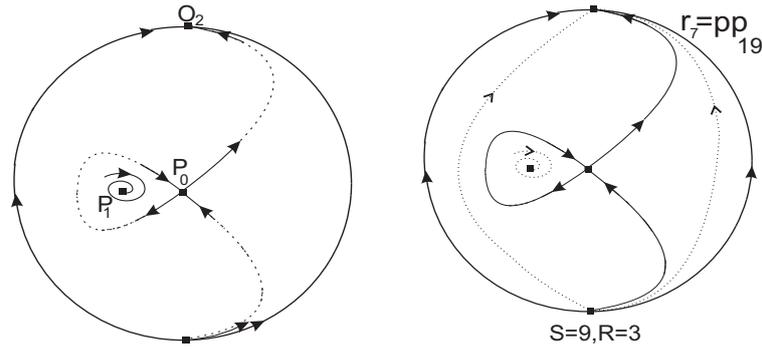
Fig. 24: The local and the global phase portraits corresponding to the region r_3.

to the global phase portrait (g). The local phase portraits (c),(d),(e_1) and (e_2) yields to the same global phase portrait (h). We summarize: For the values of the parameters in the regions $3(iii), 3(iv), 3(v), 3(vi)$ and $(3vii)$ we obtain the global phase portrait (h), see Figure 24.

Next we describe the phase portrait of system (8) corresponding to the the region r_4, see Figure 25.

(i) The unstable separatrices of the point P_1 can only have as $\omega-$ limit the points O_2 and P_-.
(ii) Consider the straight line passing through the points O_2, P_- and O_2'. Then the direction of the loop on the curve $f_2 = 0$ determines the direction of the vector field on this line, see also Lemma 10. Then the stable separatrices of P_1 can only have as $\alpha-$ limit the points P_0 and O_2'.
(iii) The unstable separatrices of P_+ have as $\omega-$ limit the points O_2 and P_-.
(iv) Finally we obtain the unique global phase portrait in the region r_4, see Figure 25.

Since by Lemma 11 system (8) have no limit cycles the phase portraits corresponding to the regions r_i for $i = 5, 6, 7, 8, 9, 10$ follow immediately from their local phase portraits, see Figures 26, 27, 28, **??**, 30
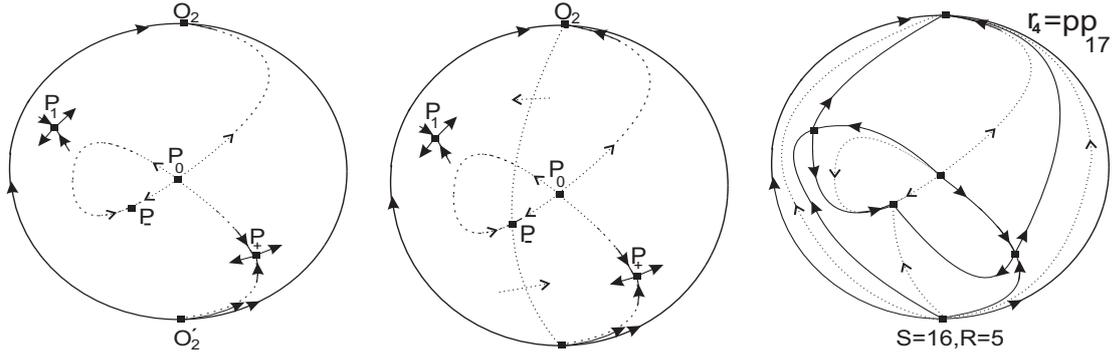
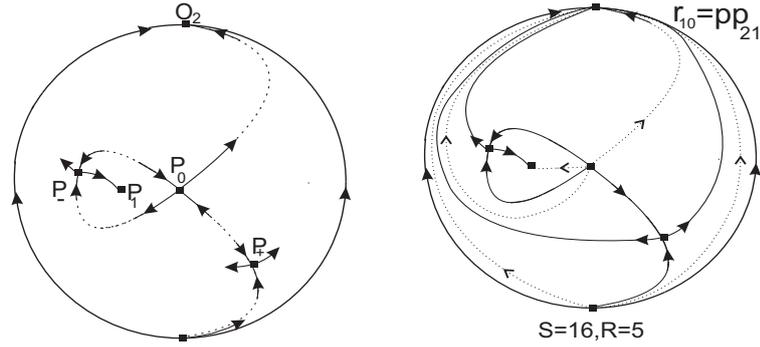Fig. 25: The local and the global phase portraits corresponding to the region r_4.

and **??**.

Fig. 26: The local and the global phase portraits corresponding to the region r_5.
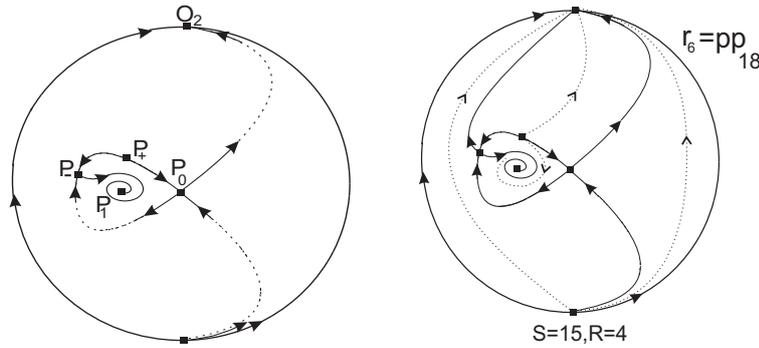
Fig. 27: The local and the global phase portraits corresponding to the region r_6.

In what follows we study the phase portrait of system (8) corresponding to the region r_{11}, see Figure 32.

(i) We consider the straight line passing through the points P_- and P_0. Note that the points Q_+, Q_- are under this straight line, and that the points Q'_+, Q'_- are upper.

(ii) The unstable separatrices of the points Q'_+ and P_- can only have as $\omega-$ limit the point O_2.

(iii) Then the unstable separatrix A of the point P_+ can only have as $\omega-$ limit the point O_2, see also Figure 32(b).

(iv) Consider the straight line passing through the points Q_+ and P_+. Then the unstable separatrix B of the

Fig. 28: The local and the global phase portraits corresponding to the region r_7.
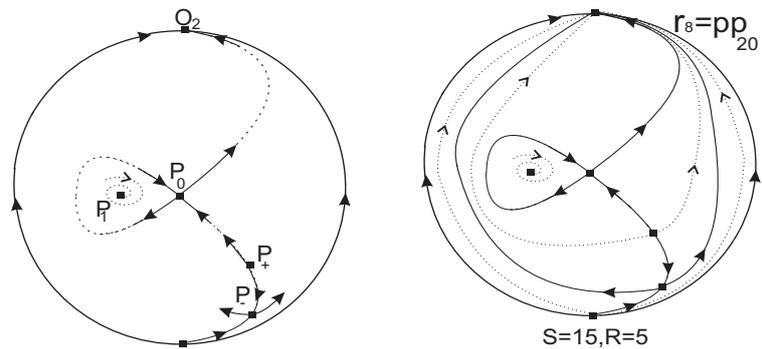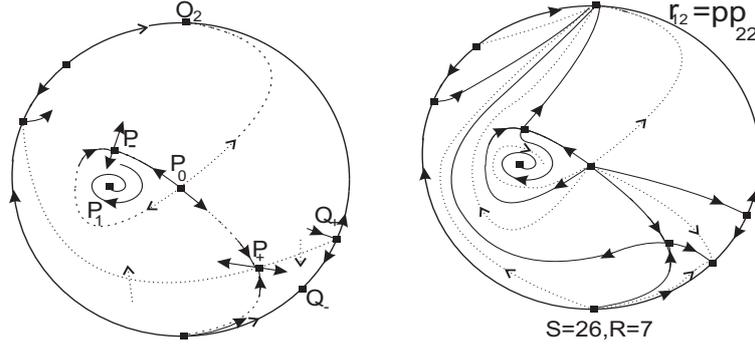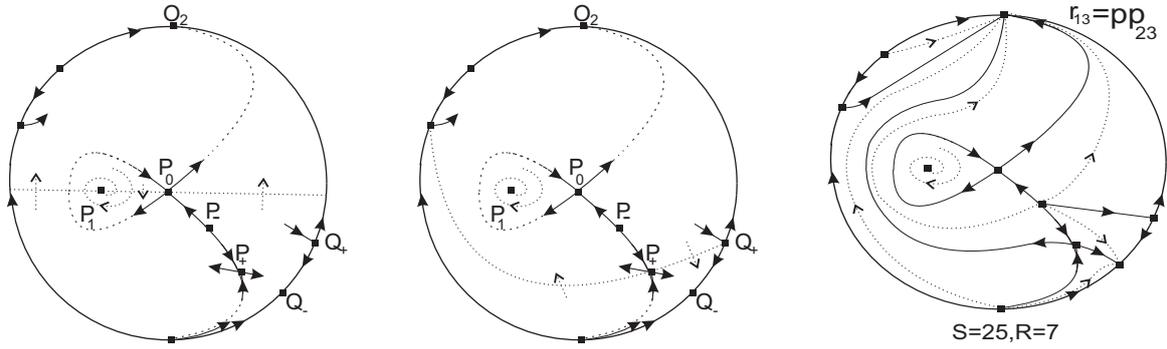

Fig. 29: The local and the global phase portrait corresponding to the region r_8.
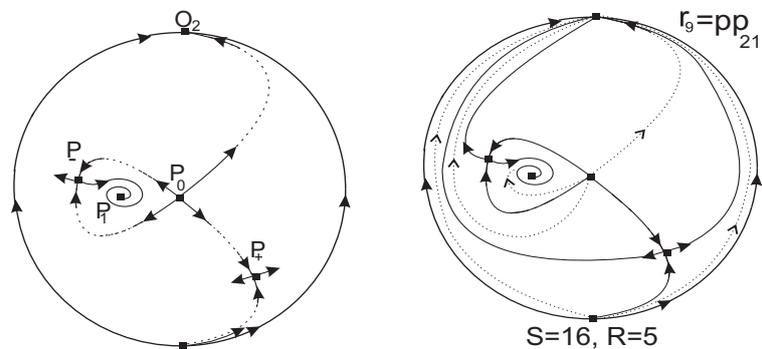
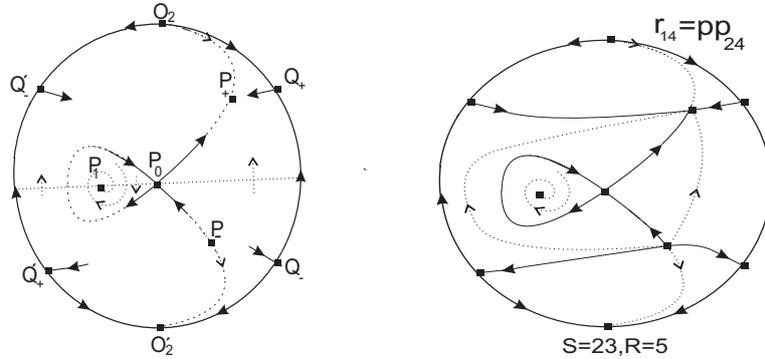Fig. 30: The local and the global phase portraits corresponding to the region r_9.

       point P_+ can only have as $\omega-$ limit the stable node Q_-, see also Figure 32(c).

(v) The stable separatrix of the point Q_+ can only have as $\alpha-$ limit the point P_0.

(vi) Finally we obtain the global phase portrait in the region r_{11}, see Figure 32(d).

       The phase portraits corresponding to regions r_{12} and r_{13} follow using the same arguments as the ones corresponding to the region r_{11} and are given in Figures **??** and 34 respectively.

       Next we describe the phase portrait of system (8) corresponding to the region r_{14}, see Figure **??**.

(i) Consider the straight line passing through the points P_0 and P_1. Note that Q_+ and Q_- are situated in the opposite sides of this straight line.

(ii) The unstable separatrices of the points Q_+ and Q'_- can only have as $\omega-$ limit the point P_+.

(iii) The stable separatrices of the points Q_- and Q'_+ can only have as $\alpha-$ limit the point P_-.

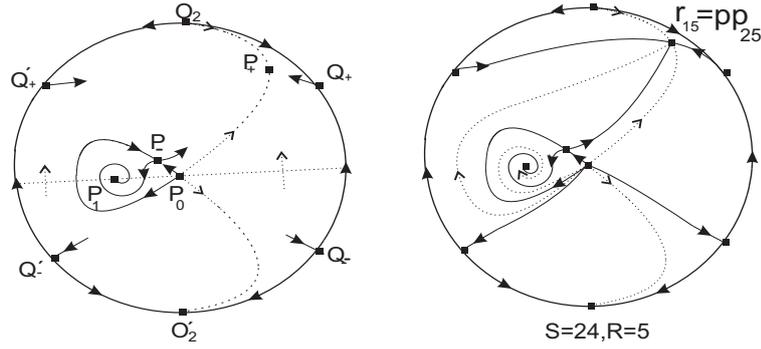(iv) Finally we obtain the global phase portrait in the region r_{14}, see Figure **??**.

Fig. 31: The local and the global phase portraits corresponding to the region r_{10}.
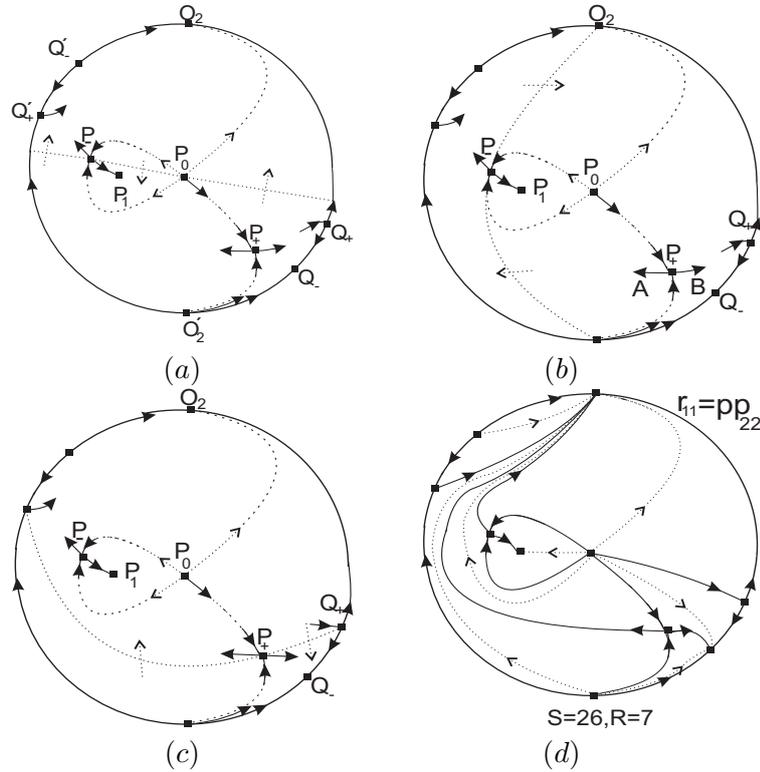
Fig. 32: The local and the global phase portraits corresponding to the region r_{11}.

The global phase portraits of system (8) in the regions r_{15} and r_{16} follow by similar arguments as in the region r_{14} and are given in Figures 36 and **??**.

Next we describe the phase portrait of system (8) corresponding to the region r_{17}, see Figure 38.

(i) Consider the straight line passing through the points Q_+, P_0 and Q'_+. In the finite region the unstable separatrix γ of the point Q_+ must be over the straight line, otherwise it must have as $\omega-$limit one of the points O'_2 or Q_-. If the point Q_- is the $\omega-$limit of γ then there is a closed path without a singular point in its interior, a contradiction. If the $\omega-$limit of γ is the point O'_2 then the stable separatrix of the point Q_- cannot have an $\alpha-$limit, a contradiction. So the direction of the vector field on the straight line is determined, see Figure 38(a)). Additionally the $\omega-$limit of γ is the point P_+. Moreover the stable separatrix of the point Q'_+ must be on the upper side of the straight line.

(ii) Consider the straight line passing through the points Q'_-, P_0 and Q_-. We distinguish the following cases for the position of the point P_1 with respect to this line:

Fig. 33: The local and the global phase portraits in the region r_{12}.

Fig. 34: The local and the global phase portraits corresponding to the region r_{13}.

Fig. 35: The local and the global phase portraits corresponding to the region r_{14}.

(ii.1) The point P_1 is below this straight line. The direction of the vector field on this straight line is as in Figure 38(b), otherwise one of the unstable separatrices of the point P_1 should have as $\omega-$ limit the point O_2'. This is a contradiction because then the stable separatrix of the point Q_+' should not have an α limit. Hence in this case the global phase portrait is given in Figure 38(c).

(ii.2) The point P_1 belongs to this straight line and so the straight line is invariant by the vector field (8). This happen when the parameters a and b satisfy equation $j_1 = 0$, see relation (9). Then the unstable separatrix of the point Q_-' can only have as $\omega-$limit the point P_1, see Figure 38(d). Then the global phase portrait is given in Figure 38(e).

(ii.3) The point P_1 is upper this straight line. Then in the finite region the unstable separatrix $\tilde{\gamma}$ of the point Q_-' must be below this straight line (see Figure 38(f)), otherwise $\tilde{\gamma}$ should have as $\omega-$limit one of the points P_+ or P_1, see Figure 38(g). If P_+ is the $\omega-$limit of $\tilde{\gamma}$ then the unstable separatrices of P_1 must go to P_+ but then the stable separatrix of P_1 has no $\alpha-$limit. So the correct direction of the vector field on

Fig. 36: The local and the global phase portraits corresponding to the region r_{15}.
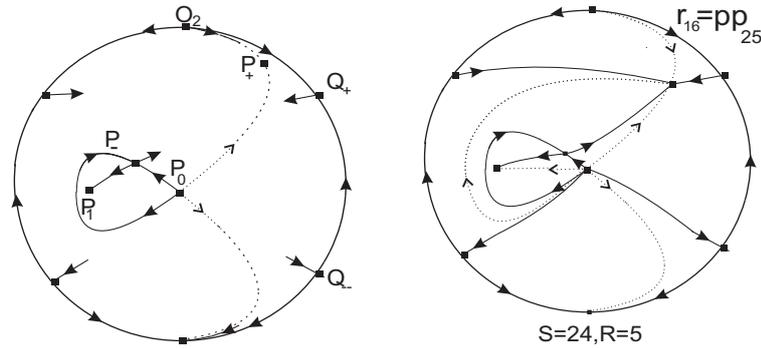
Fig. 37: The local and the global phase portraits corresponding to the region r_{16}.

the mentioned straight line is the one of Figure 38(f). Now $\tilde{\gamma}$ cannot have as $\omega-$limit the point Q'_+. So the only possible $\omega-$limit of $\tilde{\gamma}$ is the point P_-. Finally we obtain the global phase portrait, see Figure 38(h).

Next we describe the phase portrait of system (8) corresponding to the region r_{18}, see Figure 39.

(i) Consider the straight line passing through the points Q_-, P_0 and Q'_-. Note that the points P_1, P_- and P_+ in the region r_{18} are always upper this straight line, see Figure 39(a). The direction of the closed loop of the curve $f_2 = 0$ determines the direction of the vector field over this straight line, see Lemma 10. The unstable separatrix of the point Q'_- is upper this straight line and only can have as $\omega-$ limit the point P_-. Additionally the stable separatrix of the point Q_- is upper this straight line.

(ii) Now we prove that there is no connection between the separatrices of the saddles Q_+ and Q_-. If there is a conexion then in its interior should contain a singular point which must be a focus or a center, and this is a contradiction because P_1 is a node, see Theorems 2, 3 and Remark 3.3.

(iii) Consider the straight line passing through the points Q_+, P_0 and Q'_+. Note that the points P_- and P_+ are always upper this straight line. We consider the following cases for the point P_1: (iii.1) The point P_1 is upper this straight line, see Figure 39(a). Then, the unstable separatrix γ of Q_+ must be upper this straight line, otherwise either should have O'_2 as $\omega-$limit, but then the stable separatrix of the point Q_- could not have an $\alpha-$limit, a contradiction; or γ connects with the stable separatrix of Q_-, but as in (ii) this is a contradiction. This determines the direction of the vector field over this last straight line. Then γ can only have as $\omega-$limit the point P_1. (iii.2) The point P_1 belongs to this straight line, see Figure 39(b). Since this straight line is now invariant, the unstable separatix of Q_+ belongs to this line and can only have as $\omega-$limit the point P_1. (iii.3) The point P_1 is below this straight line, see Figure 39(c). Then the unstable separatrix γ of the point Q_+ can only be below this straight line. This determines the direction of the vector field over this straight line. Then again the $\omega-$limit of γ is the point P_1.

(iv) We consider the straight line passing through the points Q_-, P_+ and Q'_-. We note that on the points of the curve $h = 0$ (see relation (9)) the point P_- belongs to the straight line and system (8) has this straight
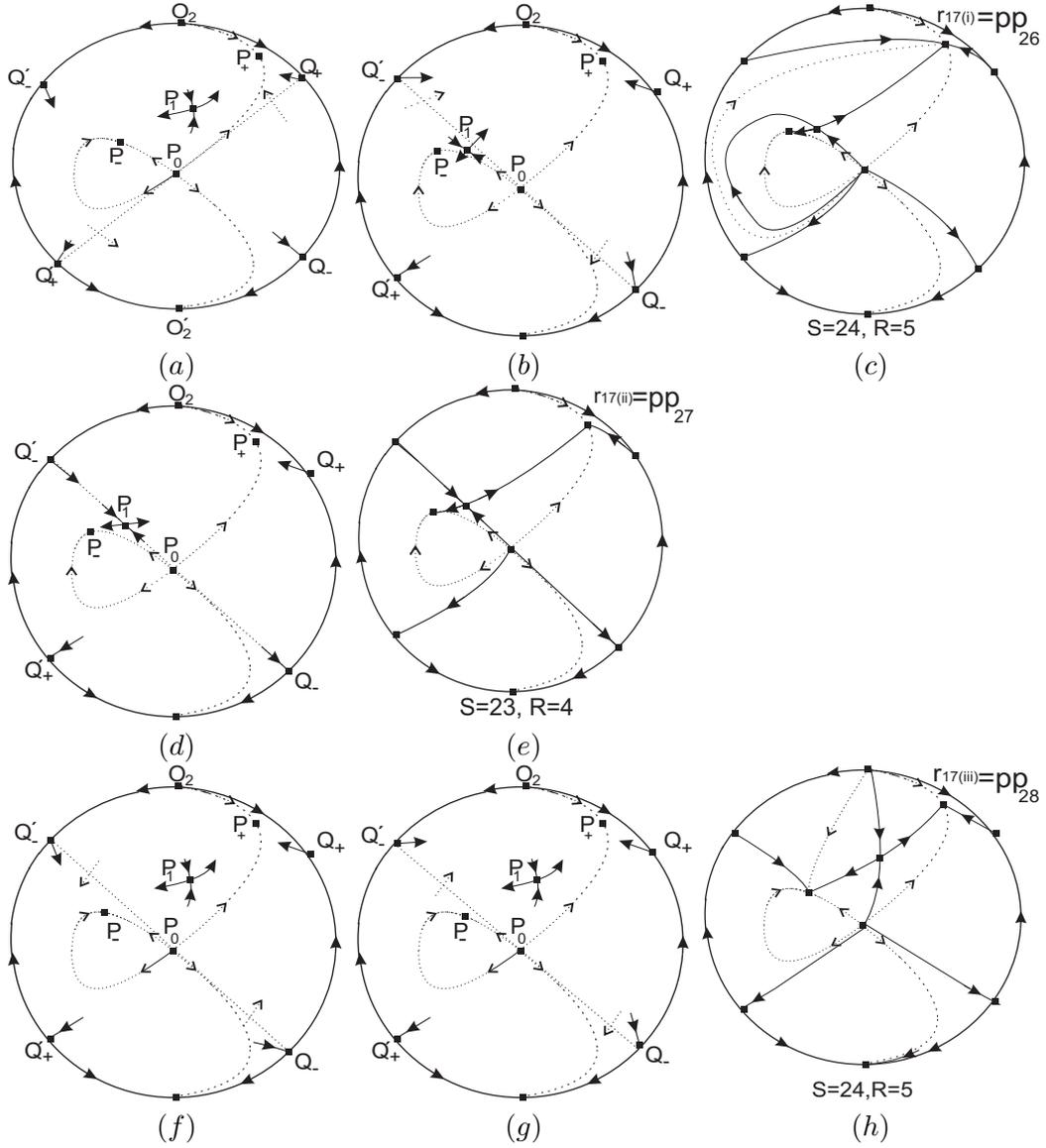
Fig. 38: The local and the global phase portraits corresponding to the region r_{17}.

line invariant. Now we distinguish three cases:

(iv.1) The point P_- is below this straight line. Then the unstable separatrices of the point P_+ have as $\omega-$ limit the points P_1 and P_-, see Figure 39(d).
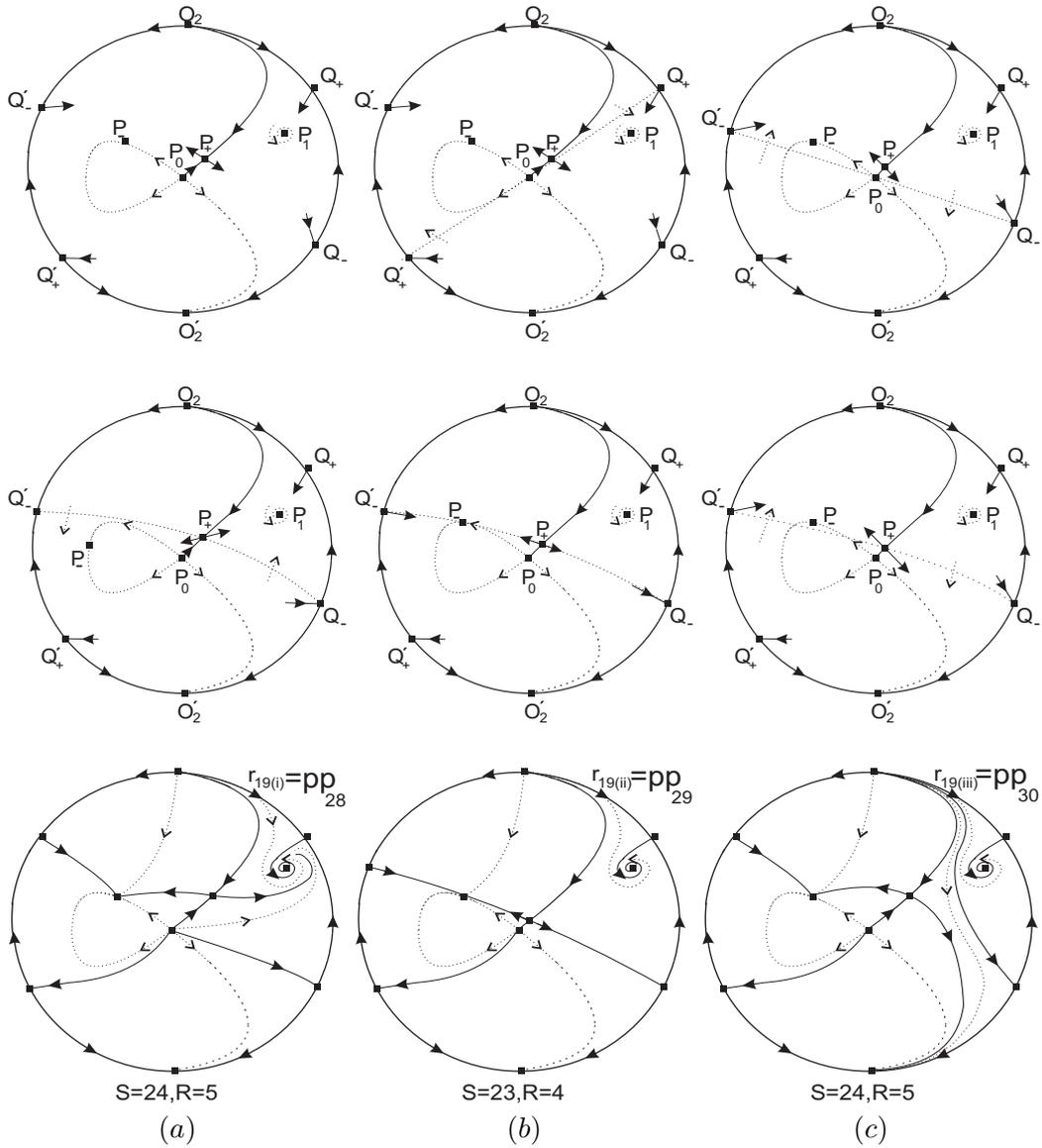
(iv.2) The point P_- belongs to this straight line. Then the unstable separatrices of the point P_+ have as $\omega-$ limit the points Q_- and P_-, see Figure 39(e).

(iv.3) The point P_- is upper this straight line. Then the unstable separatrices of the point P_+ have as $\omega-$ limit the points O_2' and P_-, see Figure 39(f).

(v) P_0 is the $\alpha-$ limit of the unstable separatrice of the point Q_+', see Figure 39(a).

(vi) Finally, we obtain the three global phase portraits in the region r_{18} see Figures 39(g),(h) and (i).

Now we study the phase portrait of system (8) corresponding to the region r_{19}, see Figure 40.

(i) Consider the straight line passing through the points Q_+, P_0 and Q_+' see Figure 40. Note that in the region r_{19} the points P_- and P_+ are always upper this straight line and the point P_1 is always below the straight line. In the finite region, the unstable separatrix γ of the point Q_+ is below the straight line, otherwise
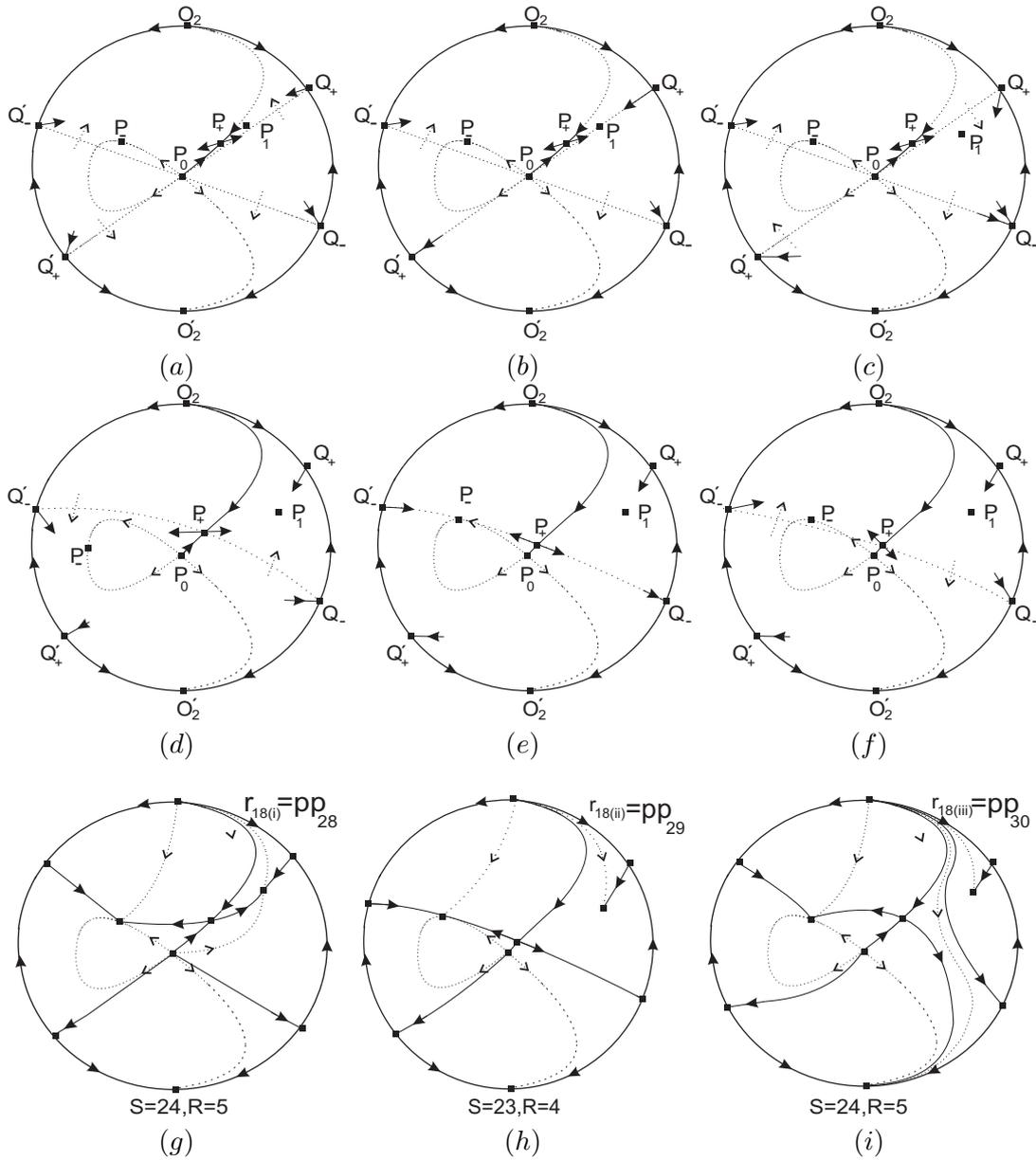
Fig. 39: The local and the global phase portraits corresponding to the region r_{18}.

could not have an $\omega-$limit. This determines the direction of the vector field over the straight line. So the $\omega-$limit of γ can only be the point P_1. The point O_2' cannot be the ω limit of γ because in this case a stable separatrix of Q_- would be without an $\alpha-$limit. Additionally there is no connection between the separatrices of Q_+ and Q_-, see Lemma 12.

(ii) Consider the straight line passing through the points Q_-, P_0 and Q_-', see Figure 40(c). Note that the point P_- is upper the straight line. Then the direction of the closed loop of the invariant curve $f_2 = 0$ determines the direction of the vector f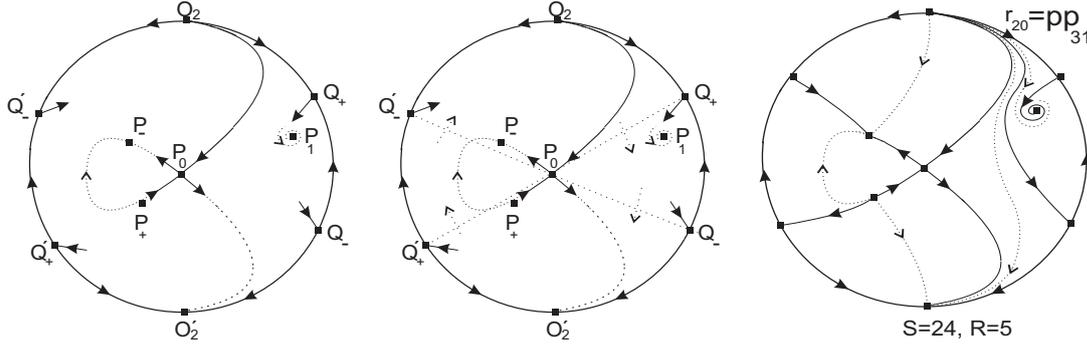ield over this straight line. The unstable separatrix of Q_-' must be over the straight line and can only have as $\omega-$limit the point P_-.

(iii) Consider the straight line passing through the points Q_+, P_+ and Q_+'. For the values of a and b that satisfy equation $h = 0$ (see relation (9)) system (8) has this straight line invariant. Hence we distinguish three cases:

(iii.1) The point P_- is below the straight line. Then the unstable separatrices of the point P_+ have as $\omega-$limit the points P_1 and P_-.

Fig. 40: The local and the global phase portraits corresponding to the region r_{19}.

(iii.2) The point P_- is on the straight line. Then the unstable separatrices of the point P_+ have as $\omega-$ limit the points Q_- and P_-. (iii.3) The point P_- is upper the straight line. Then the unstable separatrices of the point P_+ can only have as $\omega-$ limit the points O_2' and P_-.

(iv) Finally we obtain the three global phase portraits in the region r_{19} see Figures 40(a),(b) and (c).

Next we describe the phase portrait of system (8) corresponding to the region r_{20}, see Figure 41.

(i) Consider the straight line passing through the points Q_-, P_0 and Q_-'. Note that in the region r_{20} the point P_- is always upper the straight line. The direction of the closed loop of the invariant curve $f_2 = 0$ determines the direction of the vector field on this straight line. The unstable separatrix of Q_-' is upper the straight line and can only have as $\omega-$ limit the point P_-. The stable separatrix of the point Q_- is upper this straight line.

(ii) Consider the straight line passing through the points Q_+, P_0 and Q_+'. Note that in the region r_{20} the points P_+ and P_1 are always below this straight line. The direction of the closed loop of the invariant curve $f_2 = 0$ determines the direction of the vector field on this straight line. The stable separatrix of the point Q_+' is

Fig. 41: The local and the global phase portraits corresponding to the region r_{20}.

below the straight line and can only have as $\alpha-$limit the point P_+.

(iii) By Lemma 12 we have that there is no connection between the separatrices of Q_+ and Q_-. Consider the unstable separatrix γ of Q_+. Then γ cannot have O_2' as $\omega-$ limit because then the stable separatrix of Q_- will not have an $\alpha-$limit. Hence the $\omega-$limit of γ can only be the point P_1.

(iv) Finally we obtain the global phase portrait in the region r_{20}, see Figure 41.
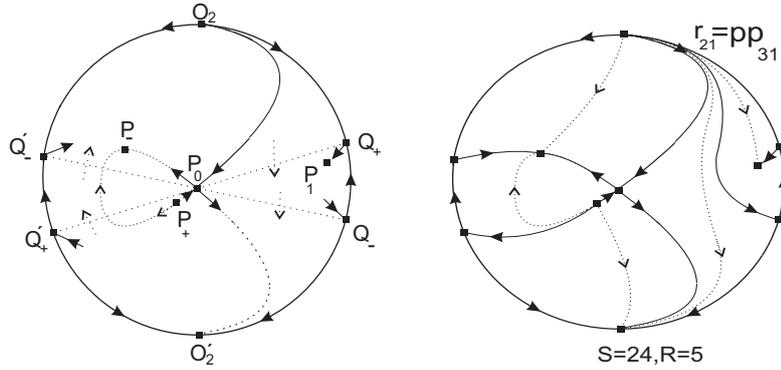
Fig. 42: The local and the global phase portraits corresponding to the region r_{21}.

In what follows we present the phase portrait of system (8) corresponding to the the region r_{21}, see Figure 42.

(i) Consider the straight line passing through the points Q_+, P_0 and Q_+'. Then in the region r_{21} the points P_1 and P_+ are always below this straight line. The stable separatrix of Q_+' can only have as $\alpha-$ limit the point P_+.

(ii) Consider also the straight line passing through the points Q_-, P_0 and Q_-'. Then in the region r_{21} the points P_- and P_1 are always upper this straight line. The unstable separatrix γ of Q_-' can have as $\omega-$ limit the point P_-.

(iii) The unstable separatrix $\tilde{\gamma}$ of Q_+ cannot have as $\omega-$ limit the point Q_- because of Theorem 2. If $\tilde{\gamma}$ has as $\omega-$ limit the point O_2' then in the finite region a stable separatrix of Q_- would be without an $\alpha-$ limit. Therefore the only possibility that remains is that $\tilde{\gamma}$ has as $\omega-$ limit the point P_1.

(iv) In the finite region the stable separatrix of Q_- must have as $\alpha-$ limit the point O_2.

(v) Finally we obtain the global phase portrait in the region r_{21}, see Figure 42.

3.4. *Phase portraits on the lines*

The bifurcation curves define 31 lines, see Figure 43. In this section we are going to present the phase portraits of system (8) in each line.
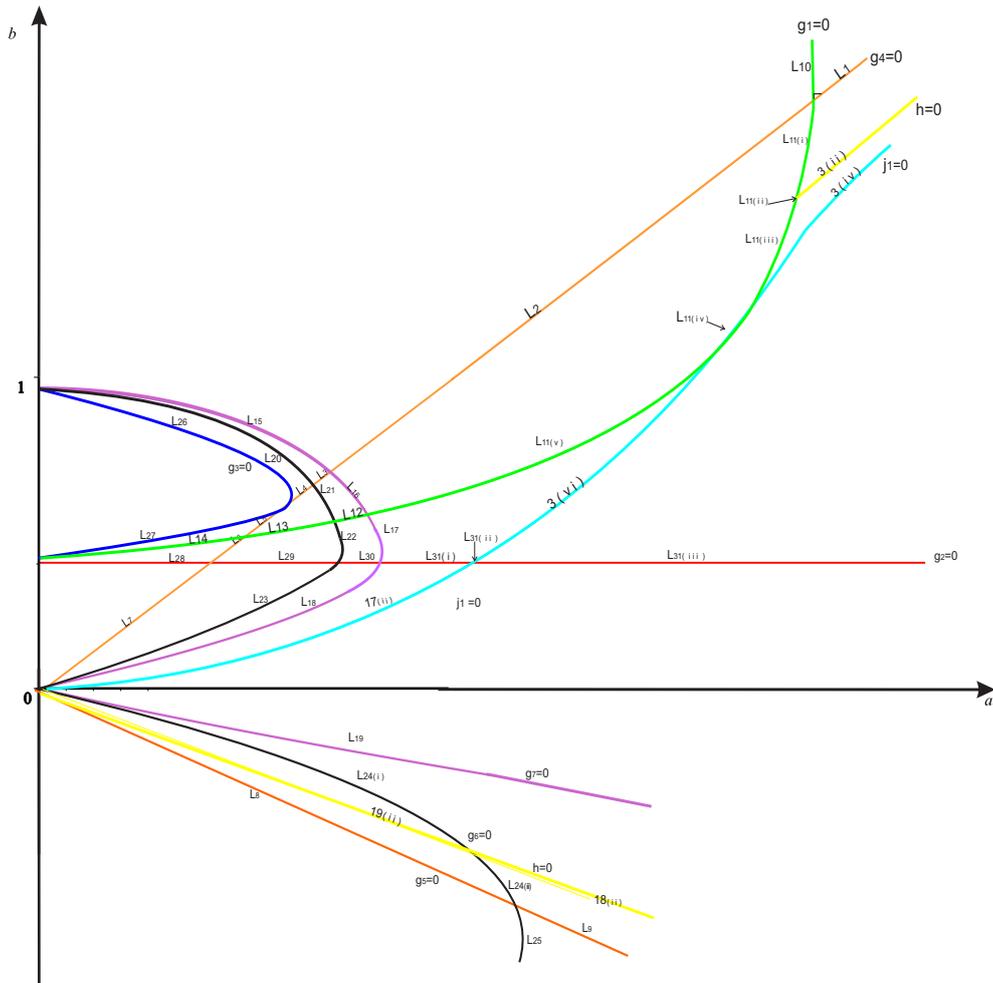
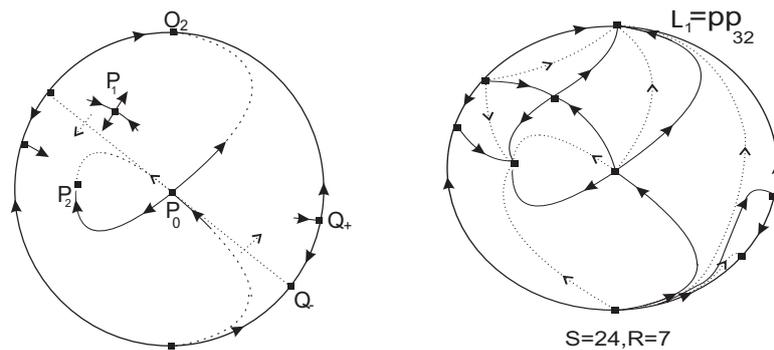Fig. 43: $c = 1, a > 0$. The bifurcation curves define 31 lines. It is a qualitative picture.

Fig. 44: The local and the global phase portraits corresponding to the line L_1.

We should provide the details for obtaining the phase portraits on the lines $L_8, L_9, L_{11}, L_{12}, L_{24}$ and L_{25}. Since the arguments used in the study of the phase portraits corresponding to these lines are the same for studying the remaining lines we only provide their phase portraits in the corresponding figures.

First we explain the phase portrait on the line L_8, see Figure 51. By Lemma 12 there is no connection between the separatrices of the points Q_1 and Q_2. Note that the unstable separatrix of the point Q_1 cannot have as $\omega-$ limit the point O_2'. In the opposite case using the continuity we should have a connection between the separatrices of the saddles. Hence, the unstable separatrix of the point Q_1 must have as $\omega-$ limit the
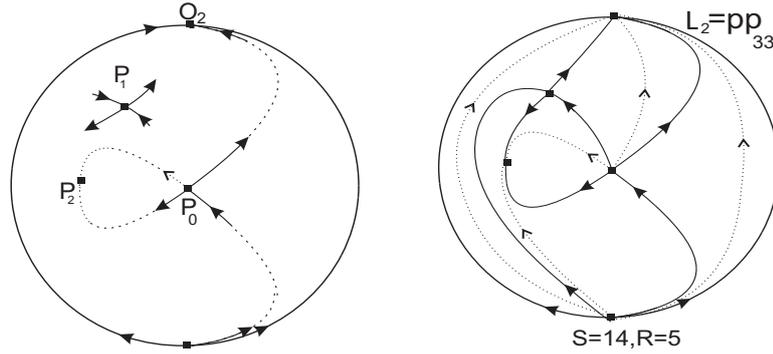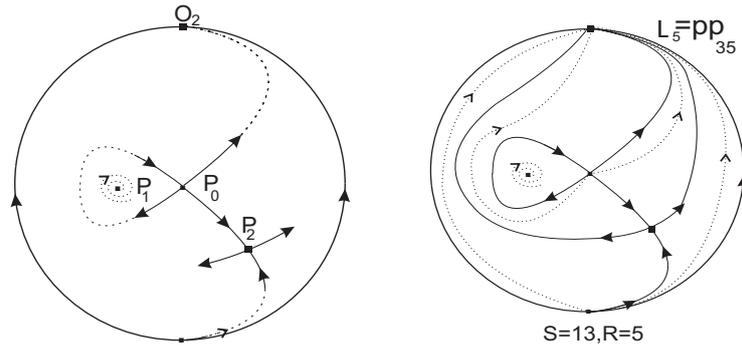
Fig. 45: The local and the global phase portraits corresponding to the line L_2.
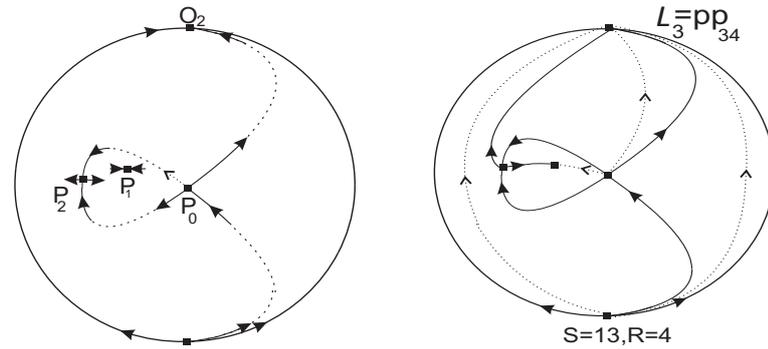
Fig. 46: The local and the global phase portraits corresponding to the line L_3.
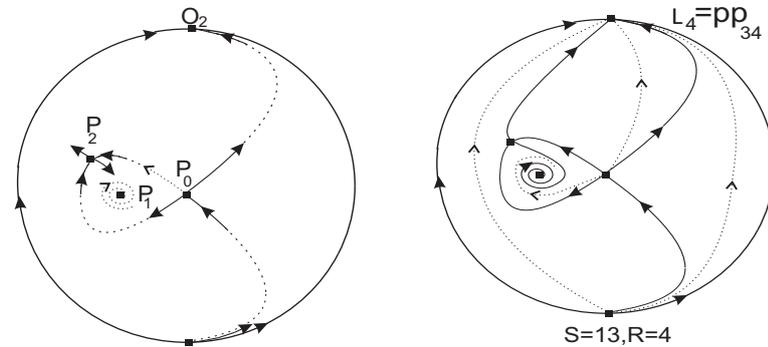
Fig. 47: The local and the global phase portraits corresponding to the line L_4.

point P_1. So on the line L_8 we obtain a unique global phase portrait, see Figure 51.

For the line L_9 note that there is no connection between the separatrices of the saddles Q_1 and Q_2. If there is a conexion then in its interior should contain a singular point which must be a focus or a center, and this is a contradiction because P_1 is a node, see Theorems 2 and 3. Now we apply similar arguments as the ones for studying the phase portrait on the line L_8 and we obtain the unique global phase portrait on the line L_9 given in Figure 52.

Now we will describe the phase portrait on the line L_{11}, see Figure 54.

(i) For $a > 4\sqrt{5}$ the point P_- is below the straight line passing through the points Q, P_+ and Q', see Figure 54, $L_{11}(i)$.
(ii) The straight line passing through the points Q, P_+ and Q' becomes invariant for $a = 4\sqrt{5}$. In this case the point P_- belong to this line, see Figure 54, $L_{11}(ii)$.
(iii) For $4 < a < 4\sqrt{5}$ the point P_- is upper the straight line passing through the points Q, P_+ and Q', see

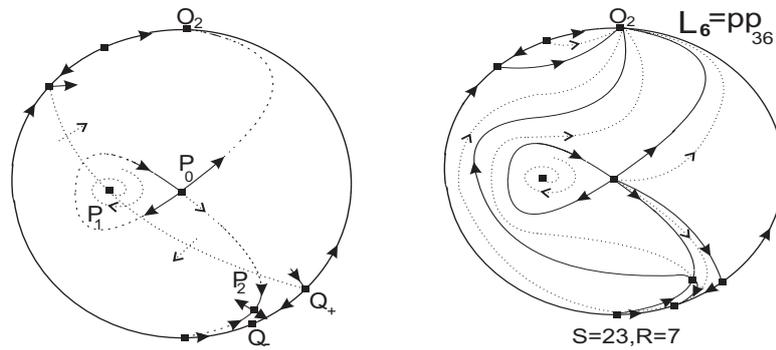Fig. 48: The local and the global phase portraits corresponding to the line L_5.

Fig. 49: The local and the global phase portraits corresponding to the line L_6.

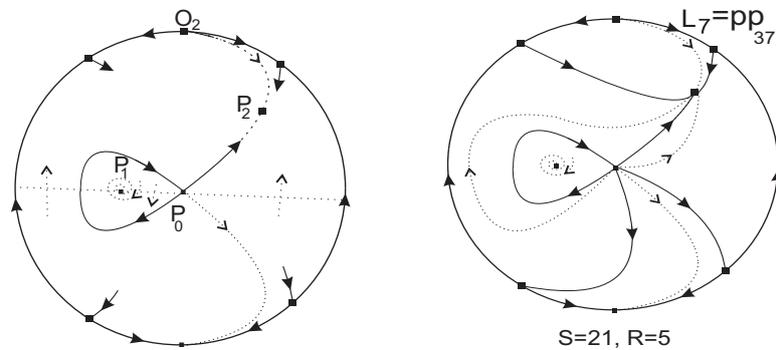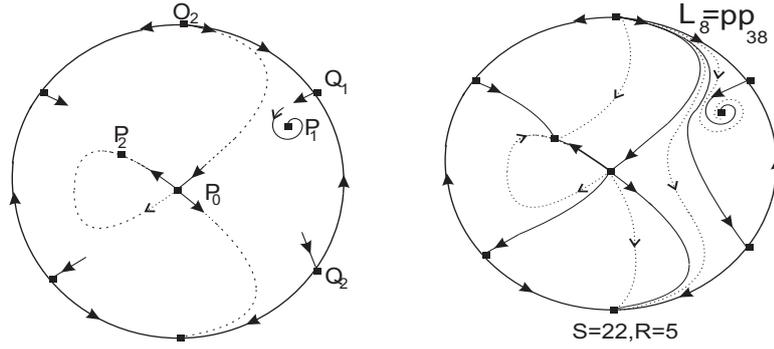

Fig. 50: The local and the global phase portraits corresponding to the line L_7.

Figure 54, $L_{11}(iii)$.

(iv) Consider the straight line passing through the points P_0, Q and Q'. For $a > 4$ the point P_1 is upper this straight line, see Figure 54, $L_{11}(i), L_{11}(ii), L_{11}(iii)$. For $a = 4$ this straight line becomes invariant. In this case the point P_1 belong to this line, see Figure 54, $L_{11}(iv)$. For $a < 4$ the point P_1 is below this straight line, see Figure 54, $L_{11}(v)$.

For the line L_{12} we consider the straight line passing through the points Q, P_+ and Q'. Note that the unstable separatrix of the point Q' determines the direction of the vector field on this line. The unique global phase portrait is given in Figure 55.

Now we are going to explain the phase portrait on the line L_{24} see Figure 67. Note that there is no connection between the separatrices of the saddles Q_1 and Q_2 because the point P_1 is a node, see Theorems 2, 3 and Remark 3.3.

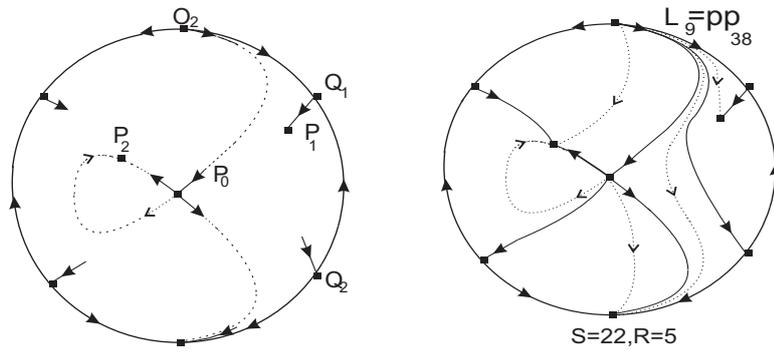Fig. 51: The local and the global phase portraits corresponding to the line L_8.

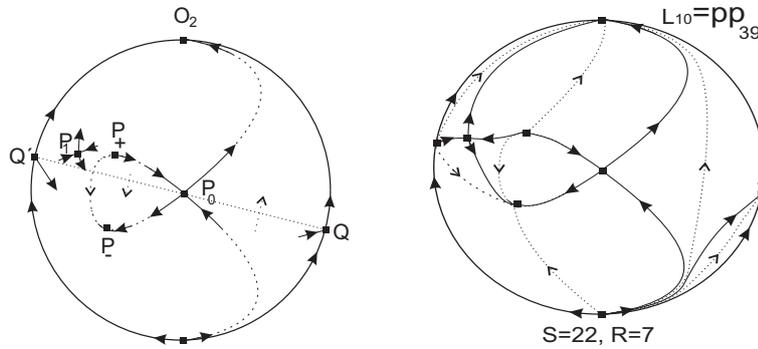Fig. 52: The local and the global phase portraits corresponding to the line L_9.

Fig. 53: The local and the global phase portraits corresponding to the line L_{10}.

Now consider the straight line passing through the points Q_2, P_+ and Q_2'. There are three possibilities:

(i) The point P_- is bellow the straight line. Then the unstable separatrix of Q_2' must be bellow the straight line, otherwise cannot have an ω–limit. This determines the direction of the vector field on the line and we obtain the global phase portrait L_{24i}.

(ii) The point P_- belongs to the straight line and the line is invariant. Then we obtain the global phase portrait L_{24ii}.

(iii) The point P_- is upper the straight line. Then the direction of the loop of the curve $f_2 = 0$ determines the direction of this straight line. Then we obtain the global phase portrait L_{24iii}.

Now we are going to explain the phase portrait on the line L_{25}, see Figure 68. If there is a connection between the separatrices of the points Q_1 and Q_2 then they form a heteroclinic loop that must contain the node, a contradiction, see Theorems 2, 3 and also Remark 3.3. Hence the unstable separatrix of the point

Q_1 must have as $\omega-$ limit the point P_1.

Note that the unstable separatrix of the point Q_1 cannot have as $\omega-$ limit the point O_2'. In the opposite case using the continuity we should have a connection between the separatrices of the saddles. So on the line L_{25} we obtain a unique global phase portrait, see Figure 68.

3.5. *Phase portraits on the intersection points*

The bifurcation curves intersect into 11 points, see Figure 75. The intersection points are described in what follows, see also Figure 75.

$$p_1 = \{g_4 = 0, g_1 = 0\} = (12 + 8\sqrt{2}, \quad 12 + 8\sqrt{2}),$$

$$p_2 = \{g_4 = 0, g_7 = 0\} = \left(\frac{8}{9}, \frac{8}{9}\right),$$

$$p_3 = \{g_4 = 0, g_6 = 0\} = \left(\frac{-68 + 8\sqrt{78}}{3}, \frac{-68 + 8\sqrt{78}}{3}\right),$$

$$p_4 = \{g_4 = 0, g_3 = 0\} = \left(\frac{4}{5}, \frac{4}{5}\right),$$

$$p_5 = \{g_4 = 0, g_1 = 0\} = (12 - 8\sqrt{2}, \quad 12 - 8\sqrt{2}),$$

$$p_6 = \{g_4 = 0, g_2 = 0\} = \left(\frac{2}{3}, \frac{2}{3}\right),$$

$$p_7 = \{g_1 = 0, g_6 = 0\} = \left(\frac{4}{3} \frac{\sqrt{(37 + 9\sqrt{318})^{1/3}(2(37 + 9\sqrt{318})^{2/3} - (37 + 9\sqrt{318})^{1/3} - 58)}}{(37 + 9\sqrt{318})^{(1/3)}}, \right.$$

$$\left. \frac{2}{27} \left(\frac{2\left(37 + 9\sqrt{318}\right)^{2/3} - \left(37 + 9\sqrt{318}\right)^{1/3} - 58}{37 + 9\sqrt{318}}\right)^{1/3} + \frac{2}{3}\right),$$

$$p_8 = \{g_1 = 0, g_7 = 0\} = \left(2 \frac{\sqrt{2}\sqrt{\sqrt[3]{13 + 16\sqrt{2}}\left(\left(13 + 16\sqrt{2}\right)^{2/3} - \sqrt[3]{13 + 16\sqrt{2}} - 7\right)}}{\sqrt[3]{13 + 16\sqrt{2}}}, \right.$$

$$\left. 1/3 \frac{\left(13 + 16\sqrt{2}\right)^{2/3} - \sqrt[3]{13 + 16\sqrt{2}} - 7}{\sqrt[3]{13 + 16\sqrt{2}}} + \frac{2}{3}\right),$$

$$p_9 = \{g_2, g_7\} = \left(\frac{2}{3}\sqrt{3}, \frac{2}{3}\right),$$

$$p_{10} = \{g_2, g_6\} = \left(\frac{4\sqrt{13}}{13}, \frac{2}{3}\right),$$

$$p_{11} = \{g_5, g_6\} = \left(\frac{68}{3} + \frac{8}{3}\sqrt{78}, \quad -\frac{68}{3} - \frac{8}{3}\sqrt{78}\right).$$

We present the phase portraits in each of these intersection points in Figures 76, 77 and 78.

4. Topological classification of the global phase portraits

Proof. [Proof of Theorem 1] In what follows we denote by S the number of separatrices and by R the number of the canonical regions. In order to present the topological classification of all global phase portraits of system (2) we apply Theorem 6 of the Appendix due to Markus, Neumann and Peixoto, see [Markus, 1954; Neumann, 1975; Peixoto, 1973] and the notion of separatrix configuration that appears there. We recall that two global phase portrait are not topological equivalent when does not exist a homeomorphism to bring the separatrix configuration of one to the separatrix configuration of the other, see again Theorem 6.

For $a = c = 0$ system (2) becomes system (3) and there is the global phase portrait pp_1 with $S = 17$ and $R = 4$.

Now for $a = 0$ and $c \neq 0$ system (2) becomes system (4) and we obtain the phase portraits given in Table 2.

Note that the phase portrait pp_2 is not topological equivalent to the phase portrait pp_4 because their separatrix configurations are not homeomorphic.

S	R	Phase portraits
19	6	pp_3
23	5	pp_2, pp_4
9	3	pp_5
12	5	pp_6
16	5	pp_7

Table 2: The phase portraits for $a = 0$.

S	R	Phase portraits
16	5	pp_8
22	5	pp_9
20	5	pp_{10}
21	4	pp_{11}
22	5	pp_{12}

Table 3: The phase portraits for $a \neq 0$ and $c = 0$.

Now we consider the case where $a \neq 0$. Because of the symmetry (5) of system (2) we can restrict our study to $a > 0$. First we consider the case where $c = 0$. So we work with system (7) and we obtain Table 3.

Note that the phase portrait pp_9 is not topological equivalent to the phase portrait pp_{12} because their separatrix configurations are not homeomorphic. For the same reason the phase portrait of pp_8 is not topologically equivalent to the phase portrait pp_7, or simply $pp_8 \neq pp_7$.

Now we consider the case where $a \neq 0$, and either $c = 0$ and $b \neq 0$, or $c \neq 0$, see Table 4.

Case $S = 9$ and $R = 3$. Then $p_4 = r_7 = pp_{19}$ and $p_4 \neq pp_5$ because in pp_5 in the interior of the loop of the curve $f_2 = 0$ we have a center whereas in p_4 we have a focus.

Case $S = 13$ and $R = 4$. We have $p_3 = L_3 = L_4 = L_{26} = pp_{34}$, $L_{15} \neq L_{26}$.

Case $S = 13$ and $R = 5$. We have $L_{27} = L_5 = pp_{35}$.

Case $S = 14$ and $R = 5$. $L_2 \neq L_{16}$.

Case $S = 16$ and $R = 5$. We obtain $r_9 = r_{10} = L_{21} = pp_{21}$, $pp_7 = r_1$, $r_9 \neq r_1$ $r_9 \neq r_4$, $r_9 \neq pp_8$ $r_4 \neq r_1$, $pp_8 \neq r_1$, $pp_8 \neq r_4$.

Case $S = 18$ and $R = 5$. There are two phase potraits $L_{31i} \neq L_{31ii}$.

Case $S = 19$ and $R = 6$. We have $L_{30} = L_{29} = pp_{53}$, $L_{29} \neq L_{31iii}$, $L_{29} \neq pp_3$, $L_{29} \neq pp_3$, $L_{29} \neq L_7$, $L_{29} \neq p_{10}$, $L_{31iii} \neq pp_3$, $L_{31iii} \neq L_7$, $L_{31iii} \neq p_{10}$, $pp_3 \neq L_7$, $pp_3 \neq p_{10}$, $L_7 \neq p_{10}$.

Case $S = 20$ and $R = 7$. The two phase portraits are $p_1 \neq p_8$.

Case $S = 21$ and $R = 6$. We have two different phase portraits $L_{11iv} \neq L_{11ii}$.

Case $S = 22$ and $R = 5$. We have $pp_{38} = L_8 = L_9 = p_{11}$, $L_8 \neq L_{19}$, $L_8 \neq L_{18}$, $L_8 \neq pp_9$, $L_8 \neq pp_{12}$, $L_{19} \neq L_{18}$, $L_{19} \neq pp_9$, $L_{19} \neq pp_{12}$, $pp_9 \neq L_{18}$, $pp_{12} \neq L_{18}$, $pp_{12} \neq pp_9$.

Case $R = 22$ and $S = 7$. We have $pp_{44} = L_{12} = L_{13} = p_7$, $L_{11iii} = L_{11v}$, $L_{11i} \neq L_{11iii}$, $L_{11i} \neq L_{12}$, $L_{11i} \neq L_{10}$, $L_{11iii} \neq L_{10}$, $L_{11iii} \neq L_{12}$, $L_{12} \neq L_{10}$.

Case $S = 23$ and $R = 4$. We have $pp_{29} = r_{18ii} = r_{19ii} = L_{24ii}$, $r_{18ii} \neq r_{17ii}$.

Case $S = 23$ and $R = 5$. We have $pp_2 \neq pp_4$, $pp_2 \neq r_{14}$, $pp_4 \neq r_{14}$.

Case $R = 24$ and $S = 5$. We have $L_{23} = r_{15} = r_{16} = pp_{25}$, $pp_{28} = r_{17iii} = r_{18i} = r_{19i} = L_{24i}$, $r_{18iii} = r_{19iii}$, $pp_{31} = r_{20} = L_{24iii} = L_{25} = r_{21}$, $r_{15} \neq r_{18i}$, $r_{15} \neq r_{18iii}$, $r_{15} \neq r_{20}$, $r_{15} \neq r_{17i}$ $r_{18i} \neq r_{18iii}$, $r_{18i} \neq r_{20}$, $r_{18i} \neq r_{17i}$, $r_{18iii} \neq r_{20}$, $r_{18iii} \neq r_{17i}$, $r_{17i} \neq r_{20}$.

Case $R = 24$ and $S = 7$. We have $L_1 \neq L_{17}$.

Case $S = 25$ and $R = 6$. We have $r_{3ii} \neq L_{22}$.

Case $S = 26$ and $R = 7$. We have $r_{11} = r_{12} = pp_{22}$, $r_2 \neq r_{3i}$, $r_2 \neq r_{3iii}$, $r_2 \neq r_{12}$, $r_{3i} \neq r_{3iii}$, $r_{3i} \neq r_{12}$, $r_{3iii} \neq r_{12}$.

In summary, we can compute 63 different topological phase portraits in the Poincaré disc for the quadratic systems (2). From these phase portraits it follows easily the proof of the statements of the

S	R	Phase portraits
9	3	$pp_5, p_4 = r_7 = pp_{19}$
10	3	$p_2 = pp_{58}$
12	5	pp_6
13	4	$p_3 = L_3 = L_4 = L_{26} = pp_{34}, L_{15} = pp_{46}$
13	5	$L_5 = L_{27} = pp_{35}$
14	5	$L_2 = pp_{33}, L_{16} = pp_{47}$
15	4	$r_5 = r_6 = L_{20} = pp_{18}$
15	5	$r_8 = pp_{20}$
16	5	$r_1 = pp_7, pp_8, r_4 = pp_{17}, r_9 = r_{10} = L_{21} = pp_{21}$
16	6	$p_6 = pp_{60}$
17	4	pp_1
17	6	$p_9 = pp_{62}$
18	5	$L_{31i} = pp_{54}, L_{31ii} = pp_{55}$
18	6	$L_{28} = pp_{52}$
19	6	$pp_3, L_{30} = L_{29} = pp_{53}, L_{31iii} = pp_{56}, p_{10} = pp_{63}$
19	7	$p_5 = pp_{59}$
20	5	pp_{10}
20	7	$p_1 = pp_{57}, p_8 = pp_{61}$
21	4	pp_{11}
21	5	$L_7 = pp_{37}$
21	6	$L_{11ii} = pp_{41}, L_{11iv} = pp_{43}$
21	7	$L_{14} = pp_{45}$
22	5	$pp_9, pp_{12}, p_{11} = L_8 = L_9 = pp_{38}, L_{18} = pp_{49}, L_{19} = pp_{50}$
22	7	$L_{10} = pp_{39}, L_{11i} = pp_{40}, L_{11iii} = L_{11v} = pp_{42}, p_7 = L_{12} = L_{13} = pp_{44}$
23	4	$r_{17ii} = pp_{27}, r_{18ii} = r_{19ii} = L_{24ii} = pp_{29}$
23	5	$pp_2, pp_4, r_{14} = pp_{24}$
23	7	$L_6 = pp_{36}$
24	5	$L_{23} = r_{15} = r_{16} = pp_{25}, r_{17i} = pp_{26}, r_{17iii} = r_{18i} = r_{19i} = L_{24i} = pp_{28}, r_{18iii} = r_{19iii} = pp_{30},$ $r_{20} = L_{24iii} = L_{25} = r_{21} = pp_{31}$
24	7	$L_1 = pp_{32}, L_{17} = pp_{48}$
25	6	$r_{3ii} = pp_{15}, L_{22} = pp_{51}$
25	7	$r_{13} = pp_{23}$
26	7	$r_2 = pp_{13}, r_{3i} = pp_{14}, r_{3iii} = pp_{16}, r_{11} = r_{12} = pp_{22}$

Table 4: The phase portraits for $a \neq 0$, and either $c = 0$ and $b \neq 0$, or $c \neq 0$.

theorem. ∎

5. Appendix

This appendix has two subsections.

5.1. *Poincaré compactification*

We consider the polynomial differential system (1) of degree m and its corresponding vector field $\mathcal{X}$. In order to plot the global phase portrait of system (1) we need to control the orbits that come or escape at infinity. For doing this control we consider the *Poincaré compactification* of system (1). For more details on this compactification see Chapter 5 of [Dumortier *et al.*, 2006].

Let $\mathbb{R}^2$ be the plane in $\mathbb{R}^3$ defined by $(y_1, y_2, y_3) = (x_1, x_2, 1)$. We define the *Poincaré sphere* $\mathbb{S}^2 = \{y = (y_1, y_2, y_3) \in \mathbb{R}^3 : y_1^2 + y_2^2 + y_3^2 = 1\}$ and we denote by $T_{(0,0,1)}\mathbb{S}^2$ the tangent space to $\mathbb{S}^2$ at the point $(0, 0, 1)$ (see [Poincaré, 1891]). We consider the central projection $f : T_{(0,0,1)} : \mathbb{R}^2 \to \mathbb{S}^2$. Note that f defines two

copies of $\mathcal{X}$, one in the northern hemisphere $\{y \in \mathbb{S}^2 : y_3 > 0\}$ and the other in the southern hemisphere. Let $\hat{\mathcal{X}} = Df \circ \mathcal{X}$ and note that $\hat{\mathcal{X}}$ is defined on $\mathbb{S}^2$ except on its equator $\mathbb{S}^1$. Then the points at infinity of $\mathbb{R}^2$ are in bijective correspondence with $\mathbb{S}^1 = \{y \in \mathbb{S}^2 : y_3 = 0\}$, (the equator of $\mathbb{S}^2$). Hence $\mathbb{S}^1$ is identified to be the infinity of $\mathbb{R}^2$. Then the *Poincaré compactified vector field* $p(\mathcal{X})$ of $\mathcal{X}$ will be analytic vector field induced on $\mathbb{S}^2$ as follows. If we multiply $\hat{\mathcal{X}}$ by the factor y_3^m, the vector field $y_3^m \hat{\mathcal{X}}$ defined in the whole $\mathbb{S}^2$.

Note that on $\mathbb{S}^2 \setminus \mathbb{S}^1$ there are two symmetric copies of $\mathcal{X}$. Hence the behavior of $p(\mathcal{X})$ around $\mathbb{S}^1$ gives the behavior of $\mathcal{X}$ near the infinity. The *Poincaré disc* $\mathbb{D}$ is the projection of the closed northern hemisphere of $\mathbb{S}^2$ on $y_3 = 0$ under $(y_1, y_2, y_3) \longmapsto (y_1, y_2)$. Moreover, $\mathbb{S}^1$ is invariant under the flow of $p(\mathcal{X})$.

Two polynomial vector fields $\mathcal{X}$ and $\mathcal{Y}$ on $\mathbb{R}^2$ are *topologically equivalent* if there exists a homeomorphism on $\mathbb{S}^2$ preserving the infinity $\mathbb{S}^1$ carrying orbits of the flow induced by $p(\mathcal{X})$ into orbits of the flow induced by $p(\mathcal{Y})$. Note that the homeomorphism should preserve or reverse simultaneously the sense of all orbits of the two compactified vector fields $p(\mathcal{X})$ and $p(\mathcal{Y})$.

Since $\mathbb{S}^2$ is a differentiable manifold we can consider the six local charts $U_i = \{y \in \mathbb{S}^2 : y_i > 0\}$, and $V_i = \{y \in \mathbb{S}^2 : y_i < 0\}$ for $i = 1, 2, 3$ with the diffeomorphisms $F_i : V_i \longrightarrow \mathbb{R}^2$ and $G_i : V_i \longrightarrow \mathbb{R}^2$, which are the inverses of the central projections from the planes tangent at the points $(1, 0, 0), (-1, 0, 0), (0, 1, 0), (0, -1, 0), (0, 0, 1)$ and $(0, 0, -1)$, respectively. Let $z = (z_1, z_2)$ be the value of $F_i(y)$ or $G_i(y)$ for any $i = 1, 2, 3$. Then the expressions of the compactified vector field $,p(\mathcal{X})$ of $\mathcal{X}$ are

$$z_2^m \Delta(z) \left(Q\left(\frac{1}{z_2}, \frac{z_1}{z_2}\right) - z_1 P\left(\frac{1}{z_2}, \frac{z_1}{z_2}\right), \; -z_2 P\left(\frac{1}{z_2}, \frac{z_1}{z_2}\right) \right) \qquad \text{in} \qquad U_1,$$

$$z_2^m \Delta(z) \left(P\left(\frac{z_1}{z_2}, \frac{1}{z_2}\right) - z_1 Q\left(\frac{z_1}{z_2}, \frac{1}{z_2}\right), \; -z_2 Q\left(\frac{z_1}{z_2}, \frac{1}{z_2}\right) \right) \qquad \text{in} \qquad U_2,$$

$$\Delta(z) \left(P(z_1, z_2), Q(z_1, z_2) \right) \qquad \text{in} \qquad U_3,$$

where $\Delta(z) = (z_1^2 + z_2^2 + 1)^{-\frac{1}{2(m-1)}}$. The expressions of the vector field $p(\mathcal{X})$ in the local chart V_i is the same as in the chart U_i multiplying by the factor $(-1)^{m-1}$. In these coordinates $z_2 = 0$ denotes the points of $\mathbb{S}^1$. We omit the factor $\Delta(z)$ by rescaling the vector field $p(\mathcal{X})$, and so we obtain a polynomial vector field in each local chart. The infinity $\mathbb{S}^1$ is invariant with $p(\mathcal{X})$.

5.2. Separatrix configuration

Let $p(\mathcal{X})$ be the Poincaré compactification in $\mathbb{S}^2$ of a polynomial vector field $\mathcal{X}$ in $\mathbb{R}^2$.

We consider the definition of parallel flows given by Markus [Markus, 1954] and Neumann in [Neumann, 1975]. Let ϕ be a $\mathcal{C}^\omega$ local flow on the two dimensional manifold $\mathbb{R}^2$ or $\mathbb{R}^2 \setminus \{0\}$. The flow (M, ϕ) is $\mathcal{C}^k$ *parallel* if it is $\mathcal{C}^\omega$-equivalent to one of the following ones:

strip: $(\mathbb{R}^2, \phi)$ with the flow ϕ defined by $\dot{x} = 1, \dot{y} = 0$;
annular: $(\mathbb{R}^2 \setminus \{0\}, \phi)$ with the flow ϕ defined (in polar coordinates) by $\dot{r} = 0, \dot{\theta} = 1$;
spiral: $(\mathbb{R}^2 \setminus \{0\}, \phi)$ with the flow ϕ defined by $\dot{r} = r, \dot{\theta} = 1$.

The *separatrices* of the vector field $p(\mathcal{X})$ in the Poincaré disc $\mathbb{D}$ are

(i) all the orbits of $p(\mathcal{X})$ which are in the boundary $\mathbb{S}^1$ of the Poincaré disc (recall that $\mathbb{S}^1$ is the infinity of $\mathbb{R}^2$);
(ii) all the finite singular points of $p(\mathcal{X})$;
(iii) all the limit cycles of $p(\mathcal{X})$; and
(iv) all the separatrices of the hyperbolic sectors of the finite and infinite singular points of $p(\mathcal{X})$.

We denote by Σ the union of all separatrices of the flow $(\mathbb{D}, \phi)$ defined by the compactified vector field $p(\mathcal{X})$ in the Poincaré disc $\mathbb{D}$. Then Σ is a closed invariant subset of $\mathbb{D}$. Every connected component of $\mathbb{D} \setminus \Sigma$, with the restricted flow, is called a *canonical region* of ϕ.

For a proof of the following result see [Li *et al.*, 2002] and [Neumann, 1975].

Theorem 5. *Let ϕ be a $\mathcal{C}^\omega$ flow in the Poincaré disc with finitely many separatrices, and let Σ be the union of all its separatrices. Then the flow restricted to every canonical region is $\mathcal{C}^\omega$ parallel.*

The *separatrix configuration* Σ_c of a flow (D, ϕ) is the union of all the separatrices Σ of the flow together with an orbit belonging to each canonical region. The separatrix configuration Σ_c of the flow (D, ϕ) is said to be *topologically equivalent* to the separatrix configuration $\tilde{\Sigma}_c$ of the flow $(D, \tilde{\phi})$ if there exists a homeomorphism from Σ_c to Σ_c which transforms orbits of Σ_c into orbits of $\tilde{\Sigma}_c$, and orbits of Σ into orbits of $\tilde{\Sigma}$.

Theorem 6. *Let (D, ϕ) and $(D, \tilde{\phi})$ be two compactified Poincaré flows with finitely many separatrices coming from two polynomial vector fields (1). Then they are topologically equivalent if and only if their separatrix configurations are topologically equivalent.*

For a proof of Theorem 6 see [Markus, 1954; Neumann, 1975; Peixoto, 1973].

In sort, in order to classify the phase portraits in the Poincaré disc of a planar polynomial differential system having finitely many separatrices, it is enough to describe their separatrix configuration.

Acknowledgments

References

J.C. Artés, R.E. Kooij & J. Llibre [1998] *Structurally stable quadratic vector fields*, Mem. Amer. Math. Soc. **134**, 108 pp.

J.C. Artés & J. Llibre [1994a] *Hamiltonian quadratic systems*, J. Diff. Eqns. **107**, 80–95.

J.C. Artés & J. Llibre [1994b] *Phase portraits for quadratic systems having a focus and one antisaddle*, Rocky Mount.J. Math. **24**, 875–889.

J.C. Artés, J. Llibre, D. Schlomiuk [2006] *The geometry of quadratic differential systems with a weak focus of second order*, Internat. J. Bifur. Chaos Appl. Sci. Engrg. **16**, 3127–3194.

J.C. Artés, J. Llibre, D. Schlomiuk & N. Vulpe [2021] *Geometric configurations of singularities of planar polynomial differential systems*, Birkhäuser, 2021.

J.C. Artés, J. Llibre & N. Vulpe [2007] *Quadratic systems with a rational first integral of degree two: a complete classification in the coefficient space $\mathbb{R}^{12}$*, Rend. Circ. Mat. di Palermo **56**, 417–444.

J.C. Artés, J. Llibre & N. Vulpe [2010] *Quadratic systems with a rational first integral of degree three: a complete classification in the coefficient space $\mathbb{R}^{12}$*, Rend. Circ. Mat. di Palermo **59**, 419–449.

J.C. Artés, J. Llibre & N. Vulpe [2009] *Quadratic systems with a polynomial first integral: A complete classification in the coefficient space $\mathbb{R}^{12}$*, J. Diff. Eqns. **246**, 3535–3558.

J.C. Artés, A.C. Rezende & R.D.S. Oliveira [2013] *Global phase portraits of quadratic polynomial differential systems with a semi–elemental triple node*, Internat. J. Bifur. Chaos Appl. Sci. Engrg. **23**, no. 8, 1350140, 21 pp.

A. N. Berlinskiĭ [1960] *On the behavior of the integral curves of a differential equation*, (Russian). Izv. Vysš. Učebn. Zaved. Matematika, (1960), **15**, 3–18.

A.N. Berlinskiĭ [1966] *Qualitative study of the differential equation $\dot{x} = x + b_0 x^2 + b_1 xy + b_2 y^2, \dot{y} = y + a_0 x^2 + a_1 xy + a_2 y^2$* J. Diff. Eqns, (1966), **2**, 174–178.

R. Bix [2006] *Conics and cubics. A concrete introduction to algebraic curves*, Second Edition, Undergraduate Texts in Math., Springer.

L. Cairó & J. Llibre [1997] *Phase portraits of planar semi–homogeneous vector fields*, Nonlinear Analisis, Th. Meth. & App. **29**, 783–811.

F. Chen, C. Li, J. Llibre & Z. Zhang [2006] *A uniform proof on the weak Hilbert's 16th problem for n = 2*, J. Diff. Eqns. **221**, 309–342.

W.A. Coppel [1966] *A survey of quadratic systems*, J. Diff. Eqns. **2**, 293–304.

S.-N. Chow, C. Li & Y. Yi [2002] *The cyclicity of period annulus of degenerate quadratic Hamiltonian system with elliptic segment loop*, Erg. Th. & Dyn. Syst. **22**, 1233–1261.

B. Coll, A. Gasull & J. Llibre [1987] *Some theorems on the existence, uniqueness and nonexistence of limit cycles for quadratic systems*, J. Diff. Eqns. **67**, 372–399.

B. Coll, C. Li & R. Prohence [2009] *Quadratic perturbations of a class of quadratic reversible systems with two centers,* Disc. & Contin. Dyn. Sys. **24**, 699–729.

R.J. Dickson & L.M. Perko [1970] *Bounded quadratic systems in the plane*, J. Diff Eqns. **6**, 251–273.

F. Dumortier & C. Li [1997] *Quadratic Lienard equations with quadratic damping*, J. Diff. Eqns. **139**, 41–59.

F. Dumortier, J. Llibre & J. C. Artés [2006] *Qualitative theory of planar polynomial systems*, Springer.

A. Gasull, S. Li-Ren & J. Llibre [1986] *Chordal quadratic systems*, Rocky Mount. J. Math. **16**, 751–782.

A. Gasull & J. Llibre [1988] *On the nonsingular quadratic differential equations in the plane*, Proc. Amer. Math. Soc. **104**, 793–794.

L. Gavrilov [2001] *The infinitesimal 16th Hilbert problem in the quadratic case*, Invent. Math. **143**, 449–497.

L. Gavrilov & I. D. Iliev [2000] *Second order analysis in polynomially perturbed reversible quadratic Hamiltonian systems*, Erg. Th. & Dyn. Syst. **20**, 1671–1686.

D.D. Hua, L. Cairo, M.R. Feix, K.S. Govinder & P.G.L. Leach [1996] *Connection between the existence of first integrals and the Painlevé property in two-dimensional Lotka-Volterra and quadratic systems*, Proc. Roy. Soc. London **452**, 859–880.

M. Han and C. Yang [2005] *On the cyclicity of a 2-polycycle for quadratic systems*, Chaos, Solitons Fract. **23**, 1787–1794.

W. Li, J. Llibre, M. Nicolau & X. Zhang [2002] *On the differentiability of first integrals of two dimensional flows*, Proc. Amer. Math. Soc. **130**, 2079–2088.

C. Li & J. Llibre [2004] *A unified study on the cyclicity of period annulus of the reversible quadratic Hamiltonian systems*, J. Dyn. and Diff. Eqns. **16**, 271–295.

J. Llibre and J.C. Medrado [2005] *Darboux integrability and reversible quadratic vector fields*, Rocky Mountain J. Math. **35**, 1999–2057.

J. Llibre, J.S. Pérez del Río & J.A. Rodríguez [2000] *Phase portraits of a new class of integrable quadratic vector fields,* Dyn. Cont. Disc. Impulsive Syst. **7**, 595–616.

J. Llibre, R. Oliveira, C. Rodrigues [2021] *Quadratic systems with an invariant algebraic curve of degree 3 and a Darboux invariant*, Electron. J. Differential Equations, Paper No. 69, 52 pp.

J. Llibre and D. Schlomiuk [2004] *The geometry of quadratic differential systems with a weak focus of third order*, Canad. J. Math. **56**, 310–343.

C. Li and Z. Zhang [2002] *Remarks on 16th weak Hilbert problem for n=2*, Nonlinearity **15**, 1975–1992.

V.A. Lunkevich and K.S. Sibirskii [1982] *Integrals of a general quadratic differential system in cases of a center*, Diff. Eqns. **18**, 563–568.

L. Markus [1954] *Global structure of ordinary differential equations in the plane*, Trans. Amer. Math Soc. **76**, 127–148.

D.A. Neumann [1975] *Classification of continuous flows on 2–manifolds*, Proc. Amer. Math. Soc. **48**, 73–81.

R Oliveira, A.C. Rezende, D. Schlomiuk and N. Vulpe [2017], *Geometric and algebraic classification of quadratic differential systems with invariant hyperbolas*, Electron. J. Differential Equations, Paper No. 295, 122 pp.

R. Oliveira, D. Schlomiuk, A.M. Travaglini and C. Valls [2021a] *Geometry, integrability and bifurcation diagrams of a family of quadratic differential systems as application of the Darboux theory of integrability*, Electron. J. Qual. Theory Differ. Equ. 2021, Paper No. 45, 90 pp.

R. Oliveira, D. Schlomiuk, and A.M. Travaglini [2021b] *Geometry and integrability of quadratic systems with invariant hyperbolas*, Electron. J. Qual. Theory Differ. Equ. Paper No. 6, 56 pp.

M.M. Peixoto [1973] *Dynamical Systems. Proccedings of a Symposium held at the University of Bahia*, 389–420, Acad. Press, New York.

H. Poincaré [1891] *Sur l'intégration des équations différentielles du premier ordre et du premier degré I*, Rend. Circ. Mat. di Palermo **5**, 161–191.

H. Poincaré [1928] *Sur les courbes définies par une équation différentielle*, Oevres compltes, Vol.1.

J.W. Reyn [1994] *A bibliography of the qualitative theory of quadratic systems of differential equations in the plane*, Third edition. Delft University of Technology, Report 94–02, 1994.

I.G. Roset [1991] *Nonlocal bifurcation of limit cycles and quadratic differential equations in the plane* (Russian), Dissertation Kand. Phys. Mat. Samarkand University, 1991.

R. Roussarie and D. Schlomiuk [2002] *On the geometric structure of the class of planar quadratic differential systems*, Qual. Th. of Dyn. Syst. **3**, 93–121.

D. Schlomiuk and N. Vulpe [2004] *Planar quadratic vector fields with invariant lines of total multiplicity at least five*, Qual. Theory Dyn. Syst. **5**, 135–194.

D. Schlomiuk and N. Vulpe [2005] *Geometry of quadratic differential systems in the neighborhood of infinity*, J. Diff. Eqns. **215**, 357–400.

D. Schlomiuk and N. Vulpe [2008a] *Integrals and phase portraits of planar quadratic differential systems with invariant lines of at least five total multiplicity*, Rocky Mountain J. Math. **38**, 1887–2104.

D. Schlomiuk and N. Vulpe [2008b] *Integrals and phase portraits of planar quadratic differential systems with invariant lines of at least five total multiplicity*, Rocky Mountain J. Math. **38**, 2015–2075.

D. Schlomiuk and N. Vulpe [2008c] *Planar quadratic differential systems with invariant straight lines of total multiplicity four*, Nonlinear Anal. **68**, 681–715.

D. Schlomiuk and N. Vulpe [2008d] *Integrals and phase portraits of planar quadratic differential systems with invariant lines of total multiplicity four*, Bul. Acad. Stiinte Repub. Mold. Mat. 27–83.

D. Schlomiuk and N. Vulpe [2008e] *The full study of planar quadratic differential systems possessing a line of singularities at infinity*, J. Dynam. Differential Equations **20**, 737–775.

D. Schlomiuk and N. Vulpe [2010] *Global classification of the planar Lotka-Volterra differential systems according to their configurations of invariant straight lines*, J. Fixed Point Theory Appl. **8**, 177–245.

D. Schlomiuk and N. Vulpe [2012] *Global topological classification of Lotka–Volterra quadratic differential systems*, Electron. J. Differential Equations, No 64, 69 pp.

D. Schlomiuk and X. Zhang [2018] *Quadratic differential systems with complex conjugate invariant lines meeting at a finite point*, J. Differential Equations **265**, 3650–3684.

N.I. Vulpe [1983] *Affine-invariant conditions for the topological discrimination of quadratic systems with a center*, J. Diff. Eqns. **19**, 273–280.

Y.Q. Ye, S.L. Cai, L.S. Chen, K.C. Huang, D.J. Luo, Z.E. Ma, E.N. Wang, M.S. Wang & X.A. Yang [1986] *A Theory of limit cycles*, Translated from the Chinese by Chi Y. Lo. Second edition. Translations of Mathematical Monographs. **66**, Amer. Math. Soc., Providence, RI.

P. Zhang [2002] *On the distribution and number of limit cycles for quadratic systems with two foci*, Qual. Theory Dyn. Syst. **3**, 437–463.

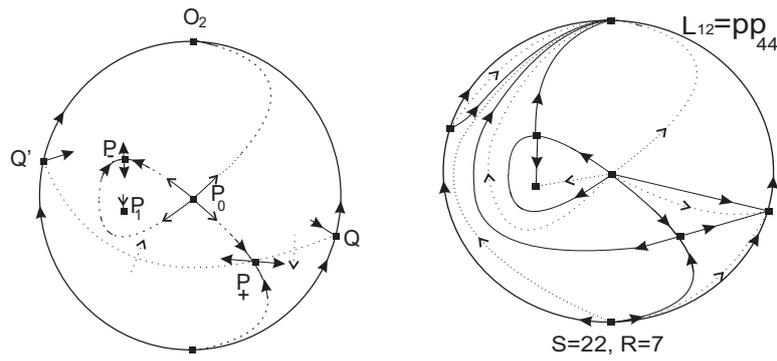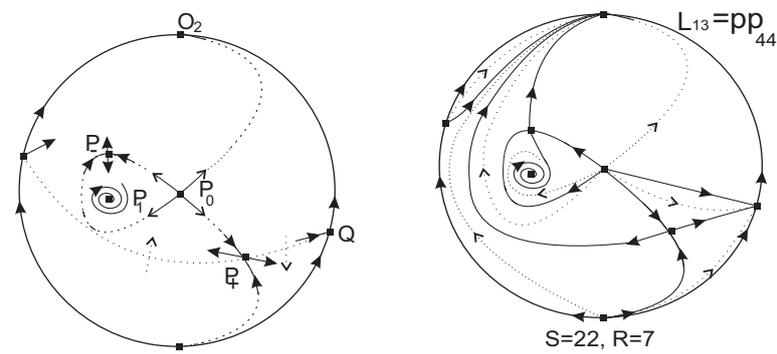H. Żołądek[1995] *The cyclicity of triangles and lines in quadratic systems*, J. Diff. Eqns. **122**, 137–159.
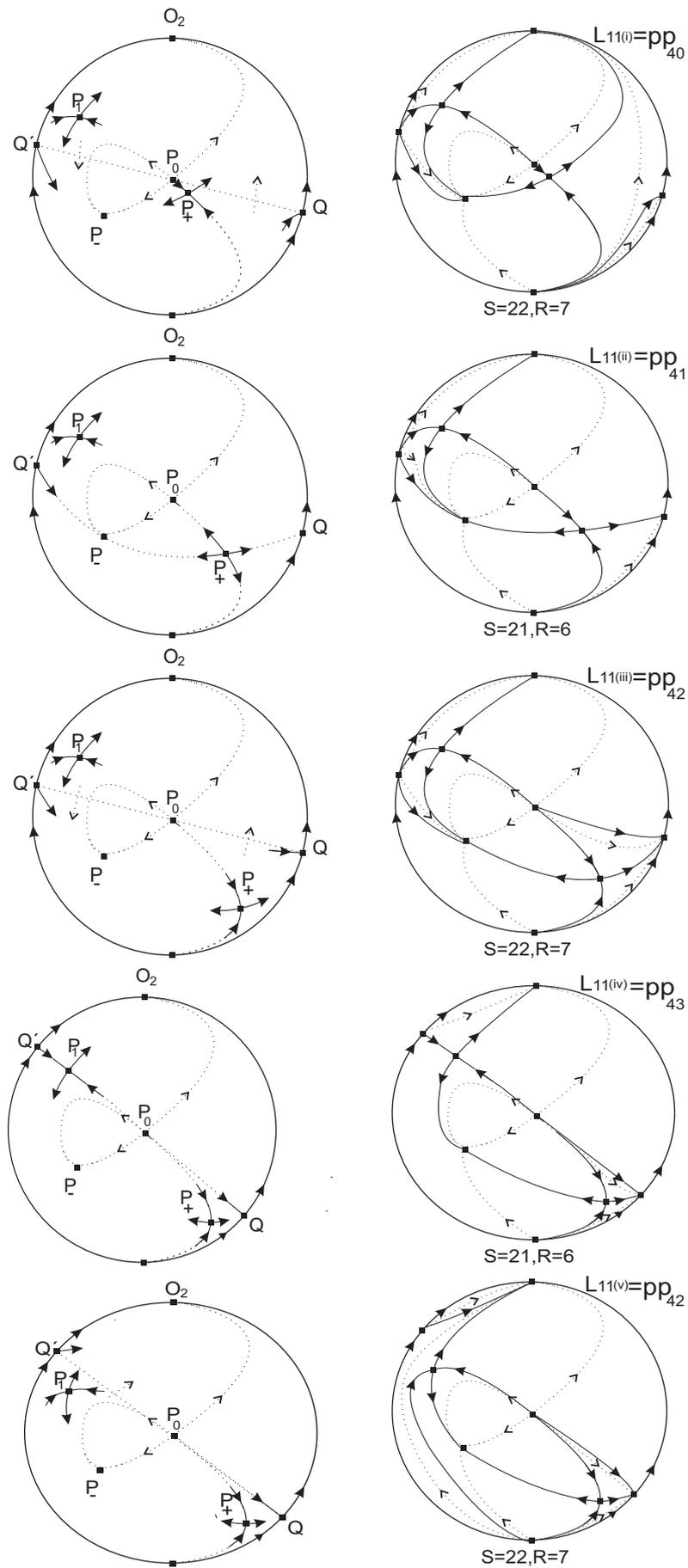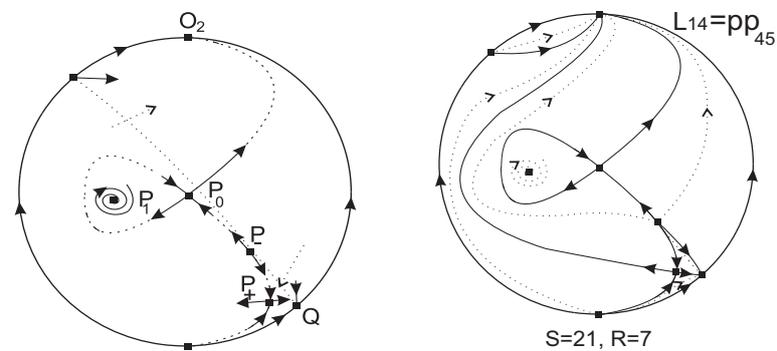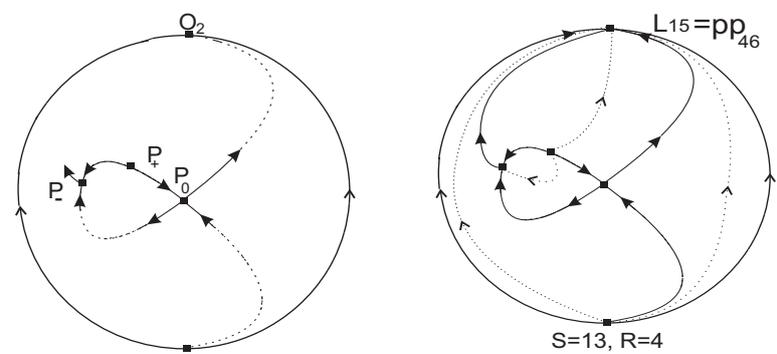
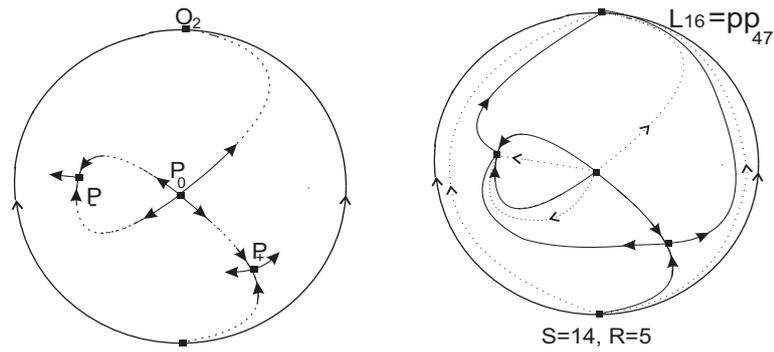Fig. 54: The local and the global phase portraits corresponding to the line L_{11}.

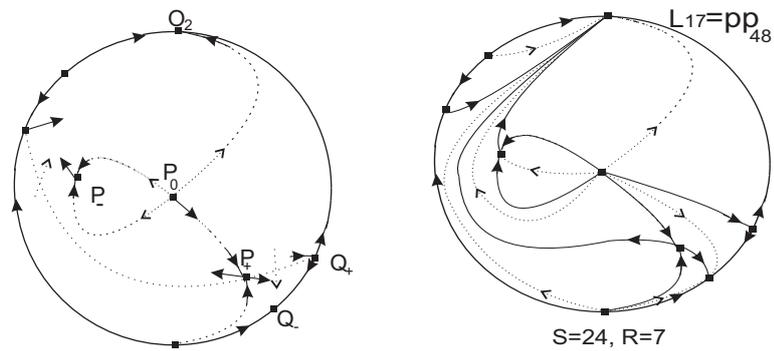Fig. 55: The local and the global phase portraits corresponding to the line L_{12}.

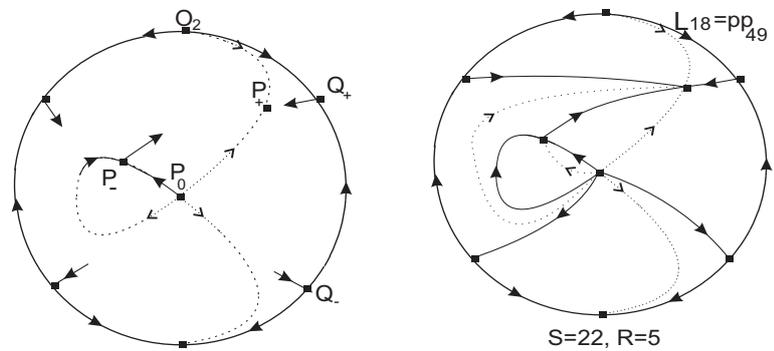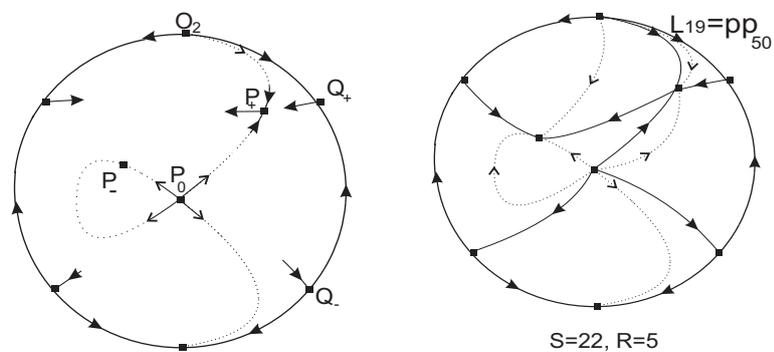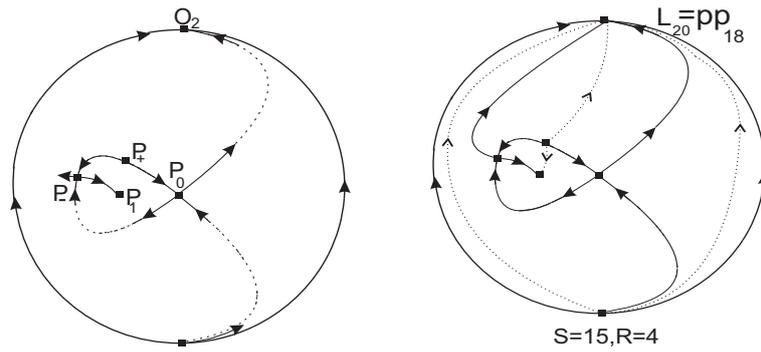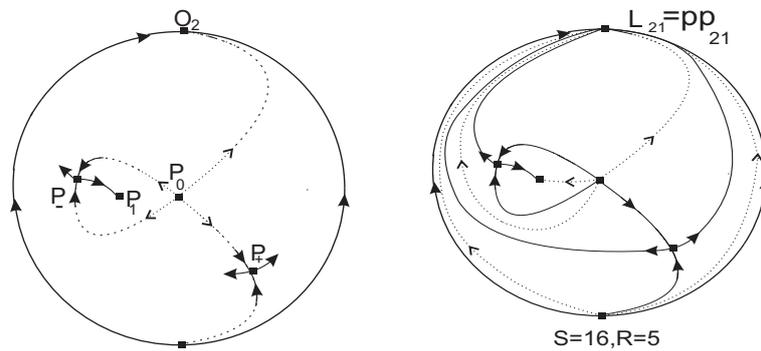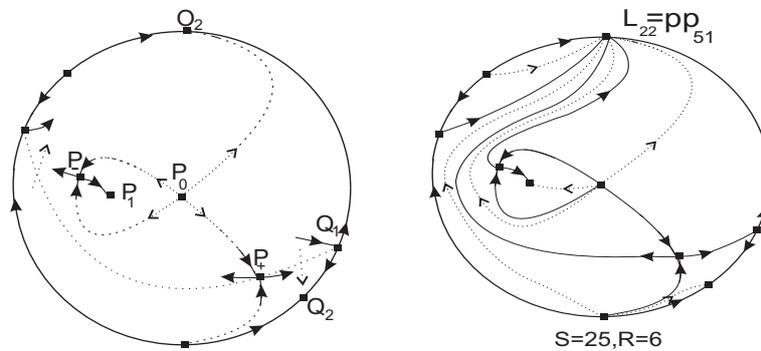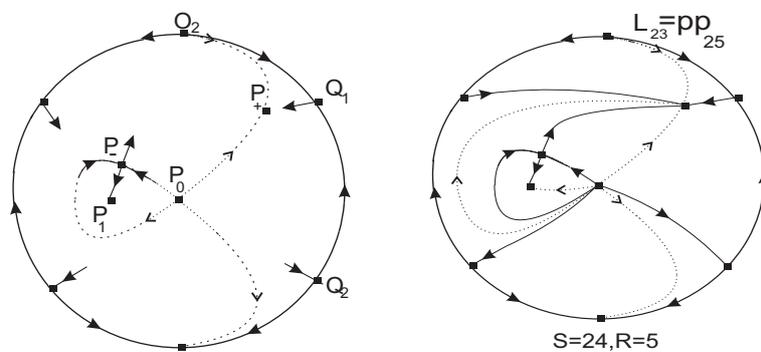Fig. 56: The local and the global phase portraits corresponding to the line L_{13}.

Fig. 57: The local and the global phase portraits corresponding to the line L_{14}.

Fig. 58: The local and the global phase portraits corresponding to the line L_{15}.

Fig. 59: The local and the global phase portraits corresponding to the line L_{16}.

Fig. 60: The local and the global phase portraits corresponding to the line L_{17}.

Fig. 61: The local and the global phase portraits corresponding to the line L_{18}.

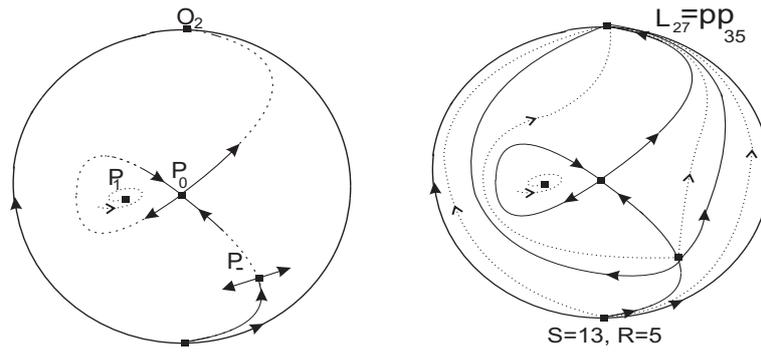Fig. 62: The local and the global phase portraits corresponding to the line L_{19}.

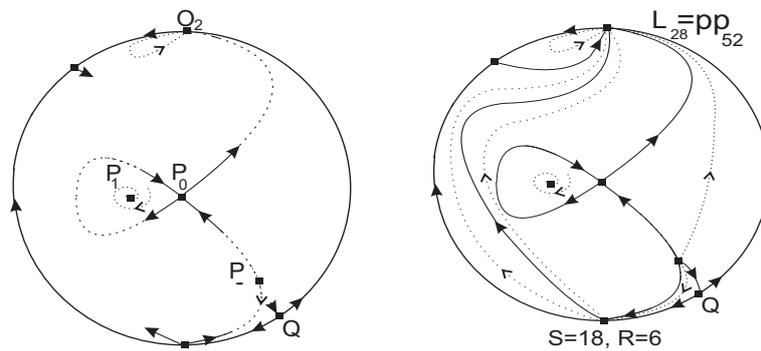Fig. 63: The local and the global phase portraits on the line L_{20}.

Fig. 64: The local and the global phase portraits on the line L_{21}.

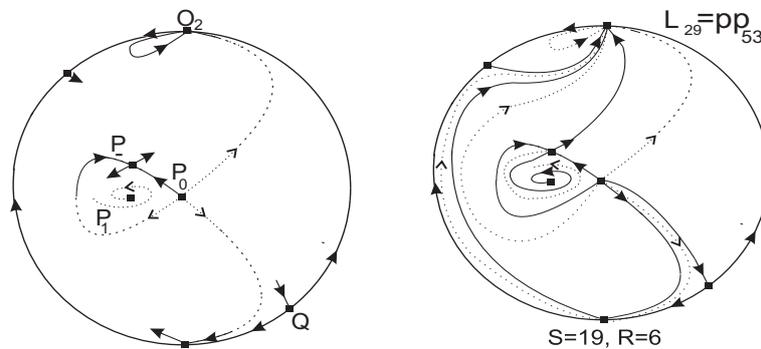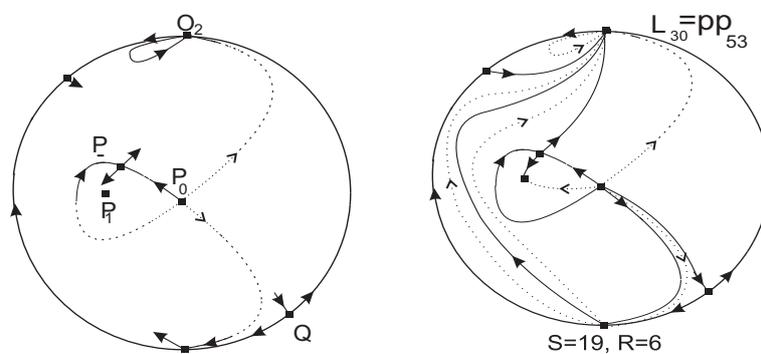Fig. 65: The local and the global phase portraits on the line L_{22}.

Fig. 66: The local and the global phase portraits on the line L_{23}.
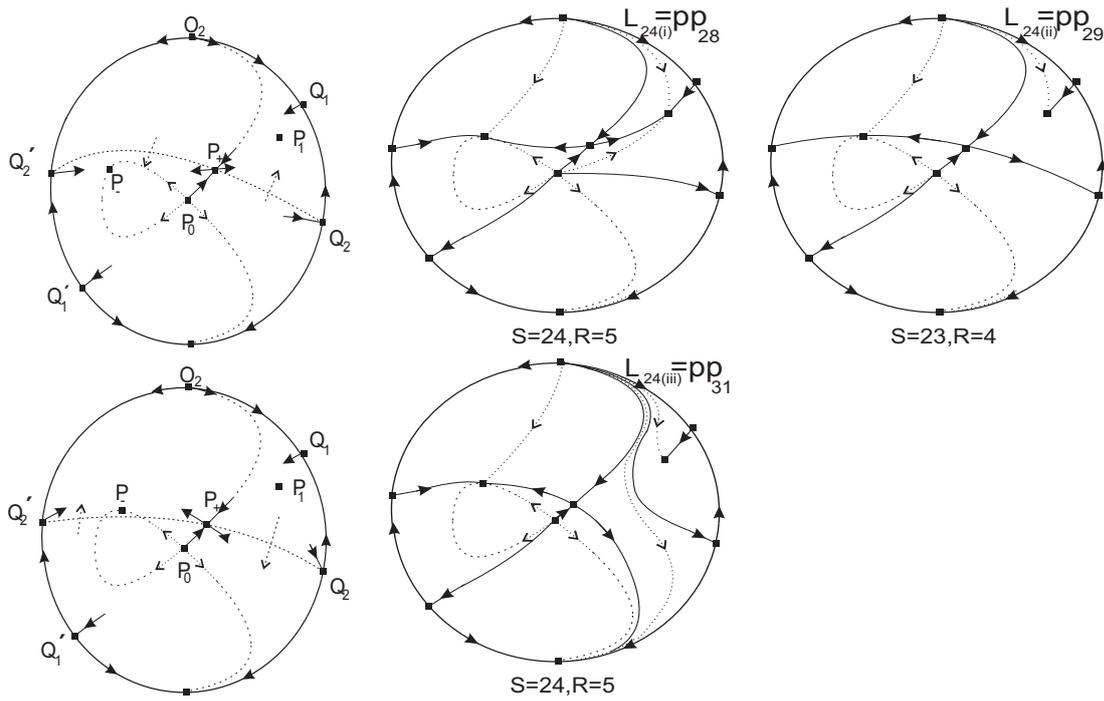
Fig. 67: The local and the global phase portraits on the line L_{24}.
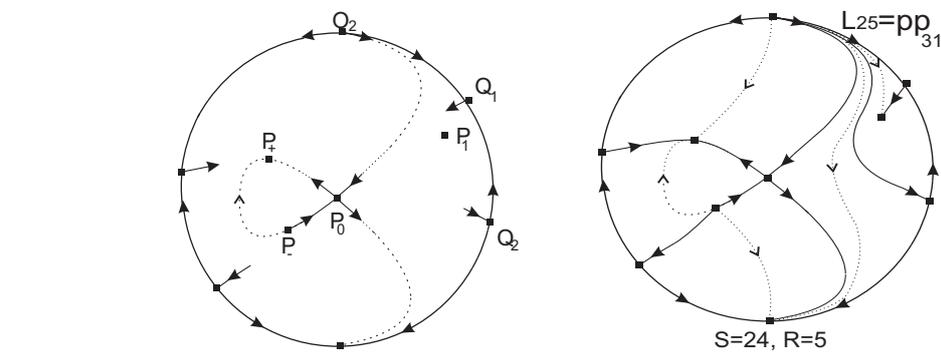
Fig. 68: The local and the global phase portraits on the line L_{25}.
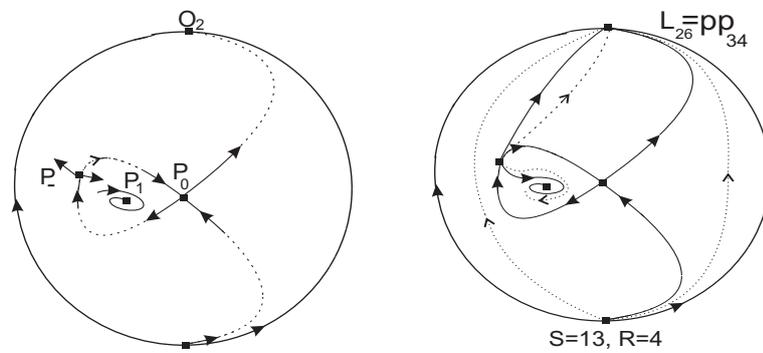
Fig. 69: The local and the global phase portraits on the line L_{26}.

Fig. 70: The local and the global phase portraits on the line L_{27}.

Fig. 71: The local and the global phase portraits on the line L_{28}.

Fig. 72: The local and the global phase portraits on the line L_{29}.

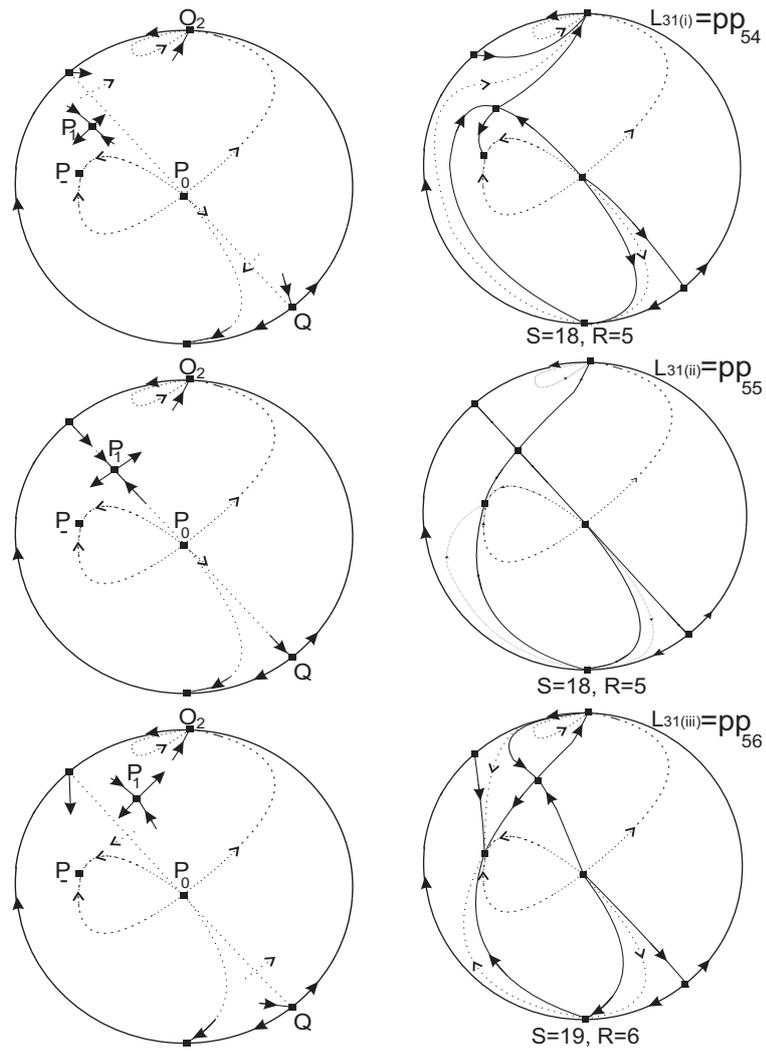Fig. 73: The local and the global phase portraits on the line L_{30}.

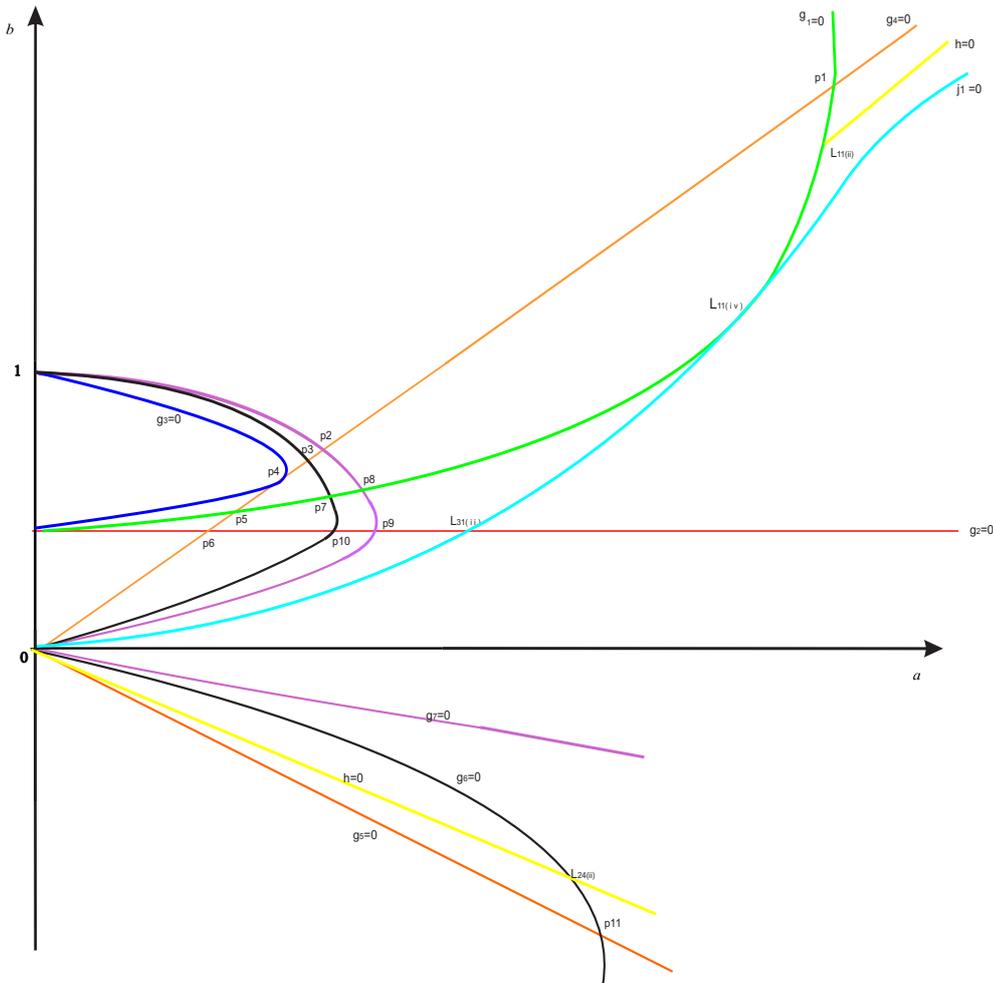Fig. 74: The local and the global phase portraits on the line L_{31}.

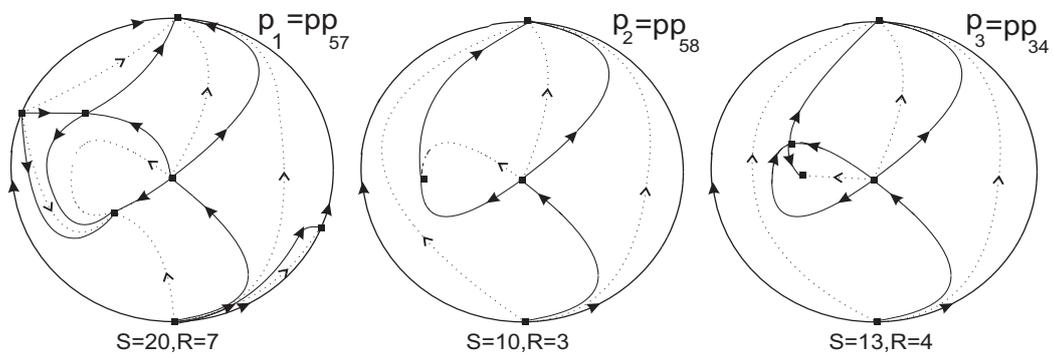Fig. 75: $c = 1, a > 0$. The bifurcation curves intersect into 11+4 points. It is a qualitative picture.

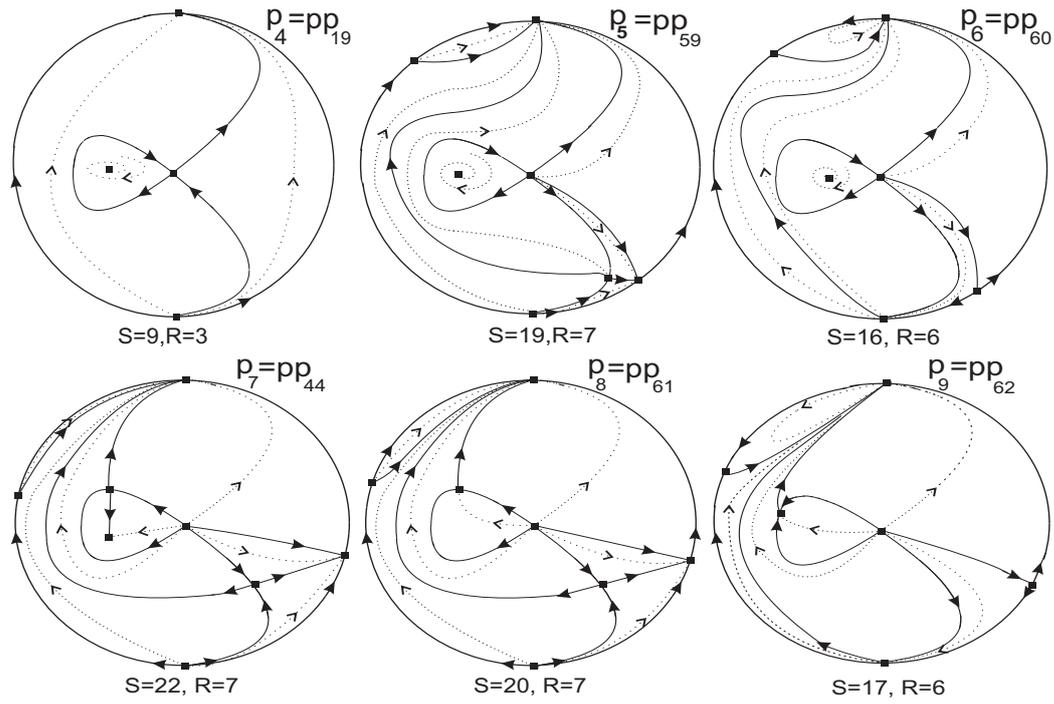Fig. 76: The phase portraits in the points p_1, p_2 and p_3.

$p_4=pp_{19}$

$p_5=pp_{59}$

$p_6=pp_{60}$

S=9,R=3

S=19,R=7

S=16, R=6

$p_7=pp_{44}$

$p_8=pp_{61}$

$p_9=pp_{62}$

S=22, R=7

S=20, R=7

S=17, R=6

Fig. 77: The phase portraits in the points p_k for $k = 4, ..., 9$.

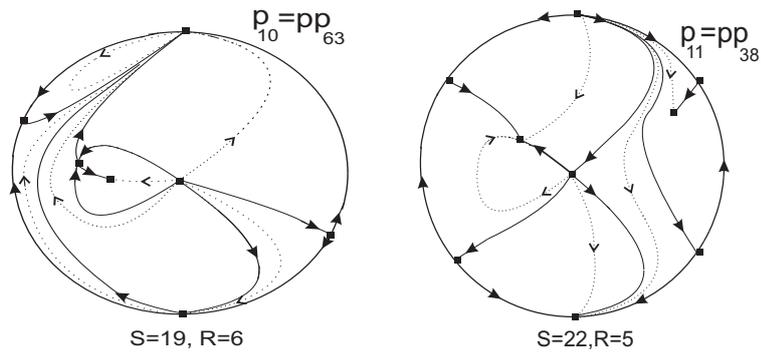$p_{10}=pp_{63}$

$p_{11}=pp_{38}$

S=19, R=6

S=22,R=5

Fig. 78: The phase portraits in the points p_{10} and p_{11}.